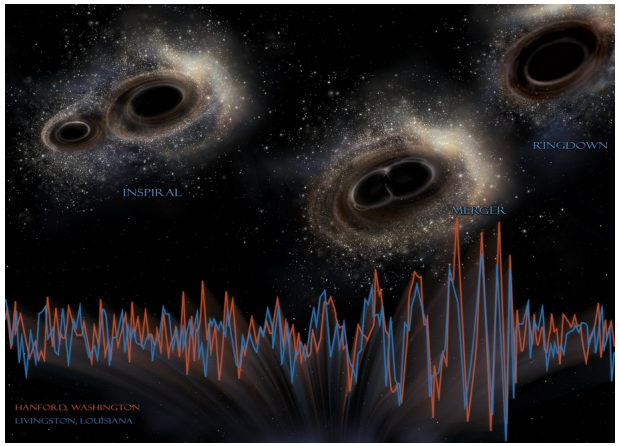

Searching for the Stochastic Gravitational-Wave Background

Varenna Course on Gravitational Waves and Cosmology

Nelson Christensen
Artemis, Observatoire de la Côte d'Azur, Nice

July 7, 2017

Outline

- What is a stochastic gravitational-wave background
- How to measure the stochastic background ?
- LIGO-Virgo data analysis methods for a stochastic gravitational wave background
- Review of Advanced LIGO Observing Run 1 Observations

- Implications of the first LIGO detections on the background from BBHs

- Cosmological sources for a stochastic background
- Astrophysical sources for a stochastic backgroun

- O1 stochastic analysis and preliminary results

- Non-standard GR stochastic searches

- Future Advanced LIGO – Advanced Virgo Observing Runs, O2 Update
- LISA
- Third generation gravitational wave detectors

- Conclusions

Review – Cosmic Microwave Background (CMB)

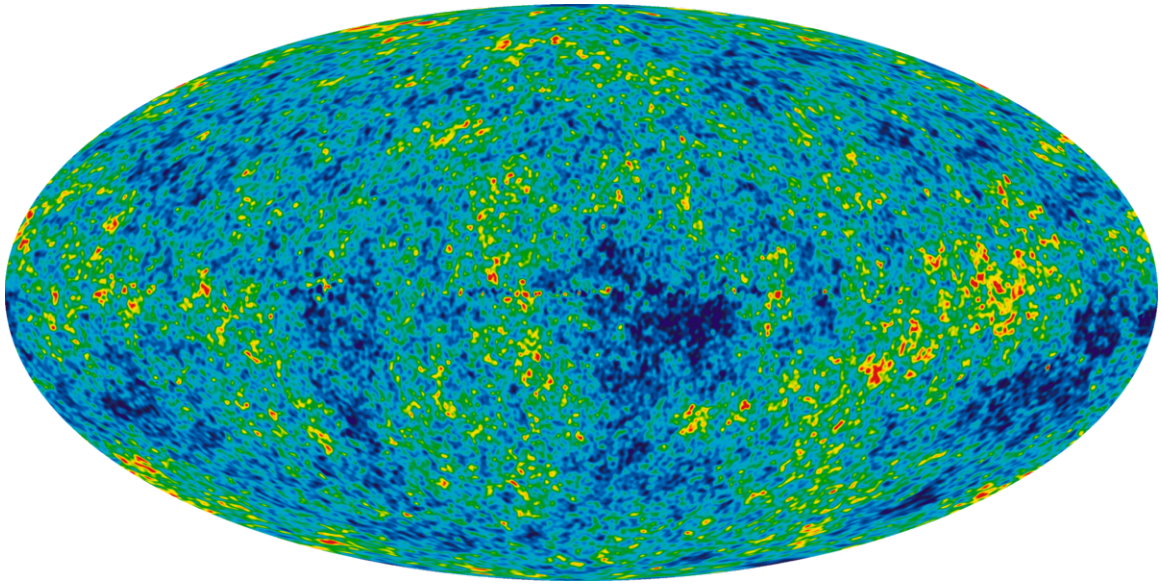

Blackbody radiation coming from every point in the sky.

Primordial plasma at 379,000 years after Big Bang, T ~ 3000 K.

Neutral hydrogen formed – universe became transparent to photons.

Universe has expanded, today T = 2.726 K, DT/T ~ 10-5

Stochastic Gravitational Wave Background (SGWB)

- Incoherent superposition of many unresolved sources.
- Cosmological:
  - » Inflationary epoch, preheating, reheating
  - » Phase transitions
  - » Cosmic strings
  - » Alternative cosmologies
- Astrophysical:
  - » Supernovae
  - » Magnetars
  - » Binary black holes
- Potentially could probe physics of the very-early Universe.

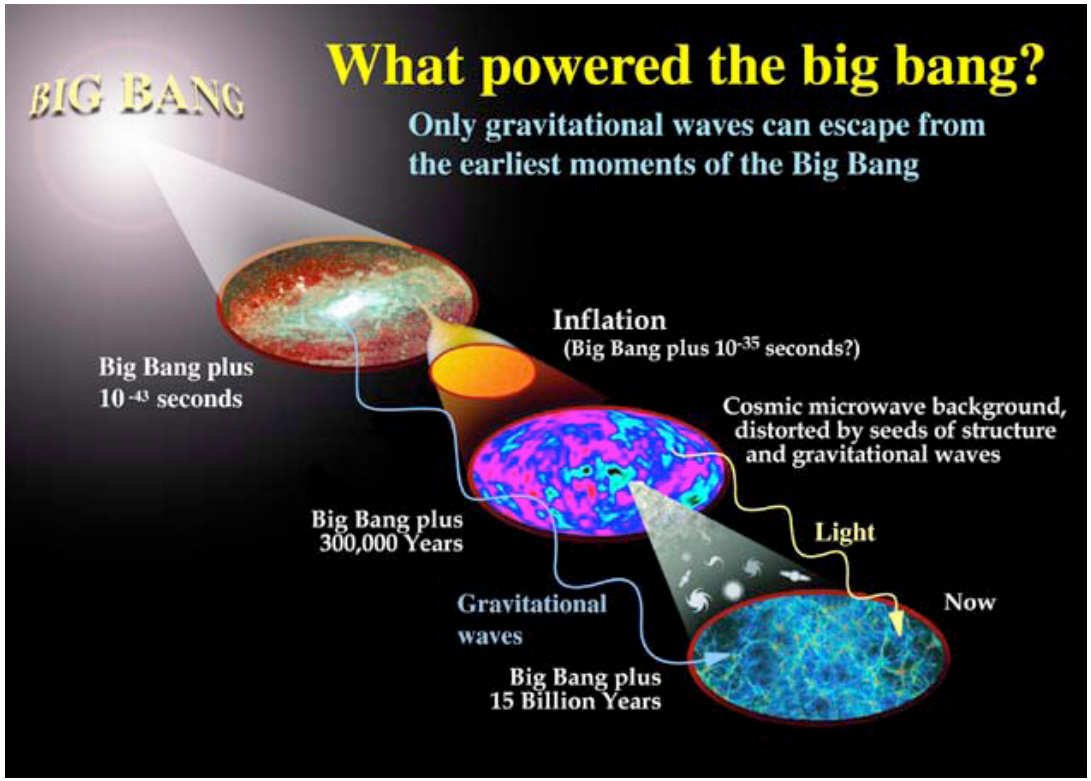

$$\Omega_{GW}(f) = \frac{f}{\rho_c}\frac{d\rho_{GW}}{df} \qquad \Omega_{GW}(f) = A(f/f_{ref})^{\alpha}$$

Data Analysis

- Assume stationary, unpolarized, isotropic and Gaussian stochastic background
- Cross correlate the output of detector pairs to eliminate the noise

$$s_i = h_i + n_i$$

$$< s_1 s_2 > = < h_1 h_2 > + \underbrace{< n_1 n_2 >}_{0} + \underbrace{< h_1 n_2 >}_{0} + \underbrace{< n_1 h_2 >}_{0}$$

$$\langle s_1(t) s_2(t') \rangle = \frac{1}{T} \int_0^T s_1(t) s_2(t + \delta t) dt \quad \text{where} \quad t' = t + \delta t$$

Assumptions About The Stochastic Backrgound

- **Stationary**
- $\langle h(t)h(t')\rangle$ only depends on t-t' and not t or t'.
- In the frequency domain :

$$\langle \tilde{h}(f)\tilde{h}(f')\rangle \propto \delta(f-f')$$

- **Gaussian**
- Central Limit Theorem – a large number of independent events produces a stochastic process.
- N-point correlators reduce to sum and differences of two point correlator $\langle h(t)h(t')\rangle$

- **Isotropic**
- Like CMB – uniform across the sky.
- Like CMB, likely to have a dipole due to Earth's motion with respect to rest frame of CMB/SGWB.

Properties of the Stochastic Gravitational Wave Background

- There is an energy density associated with the SGWB.
- Critical energy density of the universe

$$h^2_{\rm rms} = \left\langle \sum_{i,j} h_{ij} h_{ij} \right\rangle = \int_0^\infty df\, S_h(f)$$

$$\rho_{\rm gw} = \int_0^\infty \rho_{\rm gw}(f) df$$

$$= \int_0^\infty \rho_{\rm gw}(\omega) d\omega\ , \quad \rho_{\rm gw}(f) = S_h(f) \frac{\pi c^2 f^2}{8G}$$

In erg/cm^3

$$\rho_c = \frac{3c^2 H_0^2}{8\pi G}$$

$$\rho_c = 1.7 \times 10^{-8}\ h_0^2\ erg/cm^3$$

$$\Omega_{\rm gw}(f) = \frac{1}{\rho_c} \frac{d\rho_{\rm gw}}{d\ln f} = \frac{f \rho_{\rm gw}(f)}{\rho_c}$$

$$\Omega_{gw}(f) = \frac{\pi^2 S_h(f) f^3}{3H_0^2}$$

$$\Omega_{GW}(f) = A(f/f_{ref})^\alpha$$

Single Interferometer Detecting A Plane Gravitational Wave

The gravitational wave is expressed as a Fourier series. If the perturbation to the background metric is real, the gravity wave can be written as

$$h_{ij}(\mathbf{x},t)=\int \frac{d^3\mathbf{k}}{2\eta}\{e^{i(\mathbf{k}\cdot\mathbf{x}-\eta t)}[\tilde{h}_+(\hat{\mathbf{k}},\eta)e_{ij}^{+}(\hat{\mathbf{k}}) + \tilde{h}_\times(\hat{\mathbf{k}},\eta)e_{ij}^{\times}(\hat{\mathbf{k}})]+\text{c.c.}\}\ .$$

Wave vector **k**, with gravitational wave angular frequency η, $k = \eta/c$.
Sum of a large number of waves.

A plane gravitational wave at a particular frequency, from a particular location in the sky.

$$h_{ij}=[h_+e_{ij}^{+}(\hat{\mathbf{k}})+h_\times e_{ij}^{\times}(\hat{\mathbf{k}})]e^{i(\mathbf{k}\cdot\mathbf{x}-\eta t)}$$

Gravitational Waves and Laser Interferometers

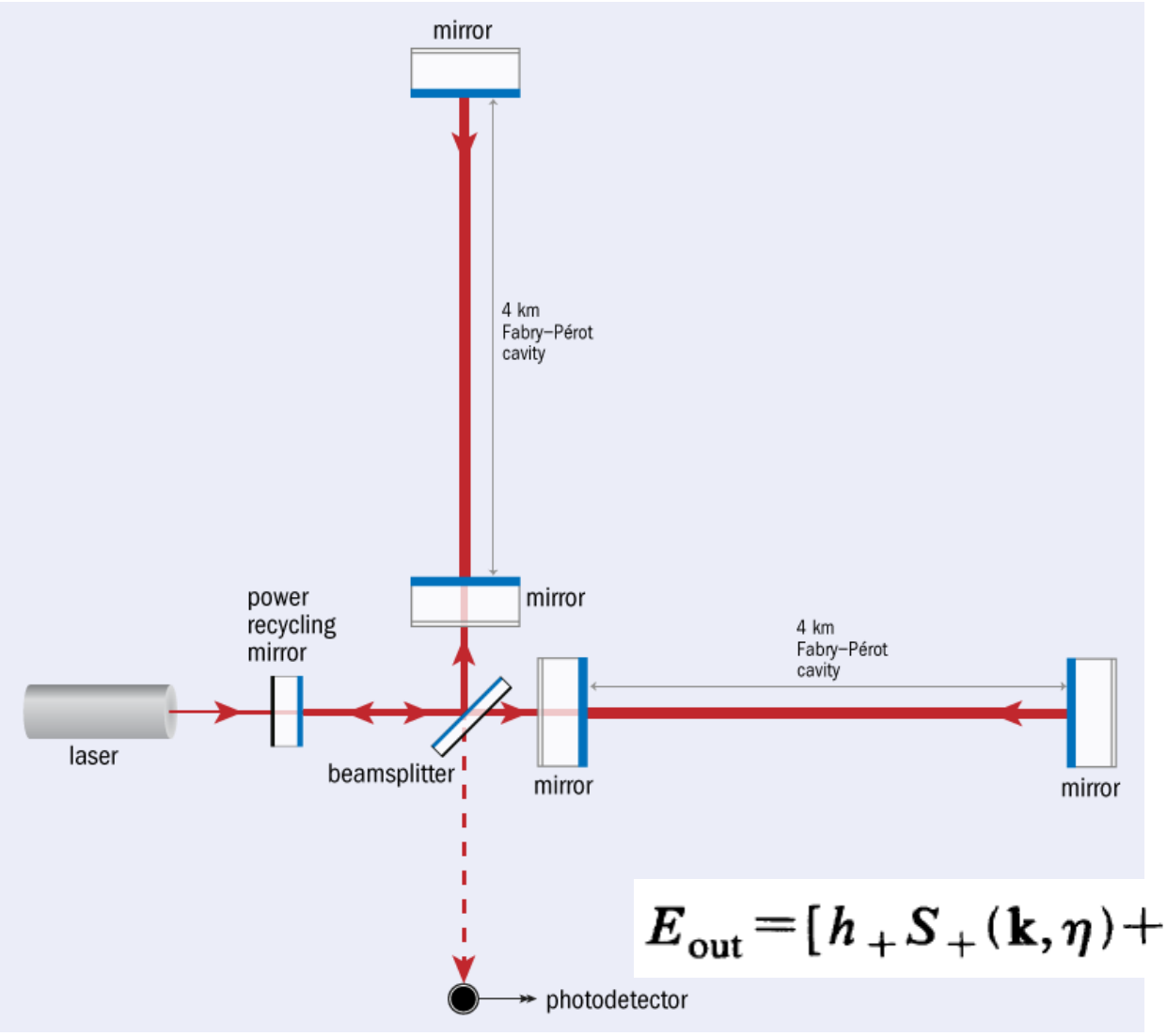

Laser with angular frequency ω.

Gravitational wave will create sidebands on output laser beam at angular frequencies
ω +/- η.

When a GW is present, there will be an electric field associated with the laser electric field at the sideband frequency.

S_+ and Sx are the transfer functions for the GW and the interferometer

$$E_{out} = [h_+ S_+(\mathbf{k},\eta) + h_\times S_\times(\mathbf{k},\eta)] E_0 e^{-i(\omega+\eta)t}$$

Gravitational Waves and Laser Interferometers

$$g_{\mu\nu}=\eta_{\mu\nu}+h_{\mu\nu}=\eta_{\mu\nu}+h_{\mu\nu}^{(+)}+h_{\mu\nu}^{(\times)} \tag{2.4}$$

and $\mathbf{k}=\{\eta/c\}\times(0,0,1)$. If the gravity wave's coordinate system is represented as (X,Y,Z) and the detector's coordinate system is (x,y,z), then the two systems are related through three Euler rotations, namely,

$$\mathbf{X}=\tilde{R}_z(-\Psi)R_x(\theta)\tilde{R}_z(-\phi)\mathbf{x}\ . \tag{2.5}$$

The relevant components of the metric in the detector's frame are

$$\begin{aligned}
h_{11}&=h_0^{(+)}e^{i(\mathbf{k}\cdot\mathbf{x}-\eta t)}[\cos2\Psi(\cos^2\phi-\cos^2\theta\sin^2\phi)-\sin2\Psi\sin2\phi\cos\theta]\\
&\quad+h_0^{(\times)}e^{i(\mathbf{k}\cdot\mathbf{x}-\eta t)}[\sin2\Psi(\cos^2\phi-\cos^2\theta\sin^2\phi)+\cos2\Psi\sin2\phi\cos\theta]\\
&\equiv[A(\theta,\phi,\Psi)h_0^{(+)}+B(\theta,\phi,\Psi)h_0^{(\times)}]e^{i(\mathbf{k}\cdot\mathbf{x}-\eta t)}\ ,
\end{aligned} \tag{2.6}$$

$$\begin{aligned}
h_{22}&=h_0^{(+)}e^{i(\mathbf{k}\cdot\mathbf{x}-\eta t)}[\cos2\Psi(\sin^2\phi-\cos^2\theta\cos^2\phi)-\sin2\Psi\sin2\phi\cos\theta]\\
&\quad-h_0^{(\times)}e^{i(\mathbf{k}\cdot\mathbf{x}-\eta t)}[\sin2\Psi(\cos^2\phi\cos^2\theta-\sin^2\phi)+\cos2\Psi\sin2\phi\cos\theta]\\
&\equiv[C(\theta,\phi,\Psi)h_0^{(+)}+D(\theta,\phi,\Psi)h_0^{(\times)}]e^{i(\mathbf{k}\cdot\mathbf{x}-\eta t)}\ .
\end{aligned} \tag{2.7}$$

In terms of the interferometer's coordinate system, the angles θ and ϕ describe the direction from which the wave came, while Ψ defines the polarization. In terms of the Euler angles defined here, the wave vector in the detector's frame is

$$\mathbf{k}=(\eta/c)(\sin\phi\sin\theta,\ -\cos\phi\sin\theta,\ \cos\theta)\ . \tag{2.8}$$

Gravitational Waves and Laser Interferometers

The term $B(\eta)$ is one-half the transfer function for a normally incident and optimally polarized gravity wave. $B(\eta)$ is only dependent on the frequency of the wave and the characteristics of the interferometer. For the purposes of a SGWB detection, one can make the approximation

$$S_+(\hat{\mathbf{k}},\eta) \approx B(\eta)[A - C] \,,$$
$$S_\times(\hat{\mathbf{k}},\eta) \approx B(\eta)[B - D] \,. \qquad (2.11)$$

LIGO-Virgo analysis, 10 Hz < f < 1000 Hz.
Approxomations for interferometer transfer functions break down for f > 10 kHz.

Gravitational Waves and Laser Interferometers

Let us assume that a gravity-wave interferometer has its arms along the $\hat{\mathbf{x}}$ and $\hat{\mathbf{y}}$ axes of the Earth-centered coordinate system. The gravity-wave interferometer would measure a signal with an amplitude of

$$h = \tfrac{1}{2}(h_{11} - h_{22}) , \tag{3.2}$$

$$\begin{aligned} h_{11} &= A(\theta,\phi,\Psi)h_0^{(+)} + B(\theta,\phi,\Psi)h_0^{(\times)} , \\ h_{22} &= C(\theta,\phi,\Psi)h_0^{(+)} + D(\theta,\phi,\Psi)h_0^{(\times)} , \end{aligned} \tag{3.3}$$

and so

$$\begin{aligned} h &= \tfrac{1}{2}[h_0^{(+)}(A-B) + h_0^{(\times)}(C-D)] \\ &= h_0^{(+)}F_+ + h_0^{(\times)}F_\times , \end{aligned} \tag{3.4}$$

$$\begin{aligned} F_+ &= \tfrac{1}{2}(1+\cos^2\theta)\cos 2\phi \cos 2\Psi - \cos\theta \sin 2\phi \sin 2\Psi , \\ F_\times &= \tfrac{1}{2}(1+\cos^2\theta)\cos 2\phi \sin 2\Psi - \cos\theta \sin 2\phi \cos 2\Psi . \end{aligned} \tag{3.5}$$

Gravitational Waves and Laser Interferometers

When a detector is located at some general location on the Earth, F_+ and $F_\times$ become very long and cumbersome. They are a function of the six Euler angles θ ϕ, Ψ, a, b, and g. Detector 1 would measure a strain

$$h = \tfrac{1}{2}(h_{11} - h_{22}) = \tfrac{1}{2}[h_0^{(+)}(A_1 - B_1) + h_0^{(\times)}(C_1 - D_1)]$$
$$= h_0^{(+)} F_{1+}(\theta, \phi, \Psi, a_1, b_1, g_1)$$
$$+ h_0^{(\times)} F_{1\times}(\theta, \phi, \Psi, a_1, b_1, g_1) \,. \qquad (3.6)$$

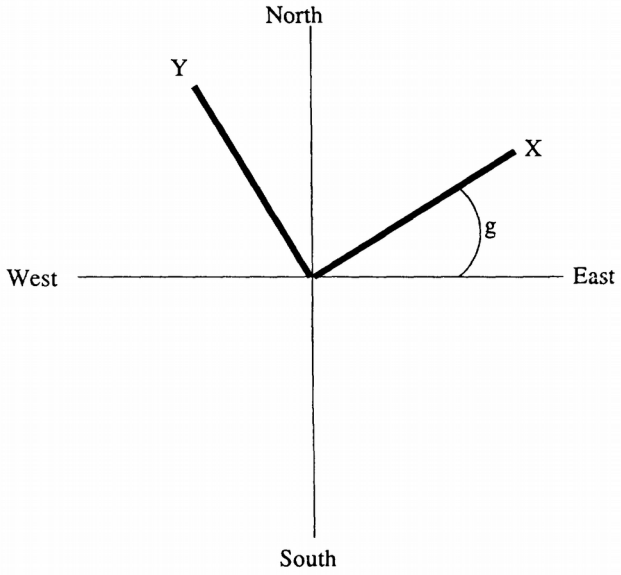

Gravitational Waves and Laser Interferometers

The gravitational-radiation background expressed as a Fourier transform is given by Eq. (2.1). The $\tilde{h}$ terms are the Fourier transforms of $h_{ij}(\mathbf{x},t)$ for each polarization. They are assumed to be stochastic random variables. Also, it is assumed that the component $h_+(\hat{\mathbf{k}},\eta)$ is uncorrelated with any other $h_+(\hat{\mathbf{k}}',\eta')$, unless $\mathbf{k}=\mathbf{k}'$. We can express this formally as

$$\langle \tilde{h}_+(\hat{\mathbf{k}},\eta)\tilde{h}_+(\hat{\mathbf{k}}',\eta')\rangle = \langle \tilde{h}_\times(\hat{\mathbf{k}},\eta)\tilde{h}_x(\hat{\mathbf{k}}',\eta')\rangle$$
$$= |\tilde{h}_0(\eta)|^2\delta^{(3)}(\mathbf{k}-\mathbf{k}') \ . \qquad (4.1)$$

$$\langle \tilde{h}_+(\hat{\mathbf{k}},\eta)\tilde{h}_\times(\hat{\mathbf{k}},\eta)\rangle = 0 \ .$$

Gravitational Waves and Laser Interferometers

$$z_1(t)=\int \frac{d^3\mathbf{k}}{2\eta}[e^{i(\mathbf{k}\cdot\mathbf{x}-\eta t)}\{\tilde{h}_+(\hat{\mathbf{k}},\eta)S_+(\hat{\mathbf{k}},\eta)+\tilde{h}_\times(\hat{\mathbf{k}},\eta)S_\times(\hat{\mathbf{k}},\eta)\}+\text{c.c.}]\ .$$

$$\langle z_1(t)z_2(t+\tau)\rangle_{\text{av}}$$

$$=\int_0^\infty \frac{d\eta\, 8G\rho_g(\eta)|B(\eta)|^2}{c^2\eta^2}\gamma(\mathbf{x}_1,\mathbf{x}_2,\eta,\tau)\ ,$$

$$\gamma(\mathbf{x}_1\mathbf{x}_2,\eta,\tau)$$

$$=\int_0^{2\pi} d\phi \int_0^{\pi}\sin\theta\, d\theta[(F_{1+}F_{2+}+F_{1\times}F_{2\times})]$$

$$\times\cos\{[\mathbf{k}\cdot(\mathbf{x}_1-\mathbf{x}_2)+\eta\tau]\}\ .$$

Overlap reduction function

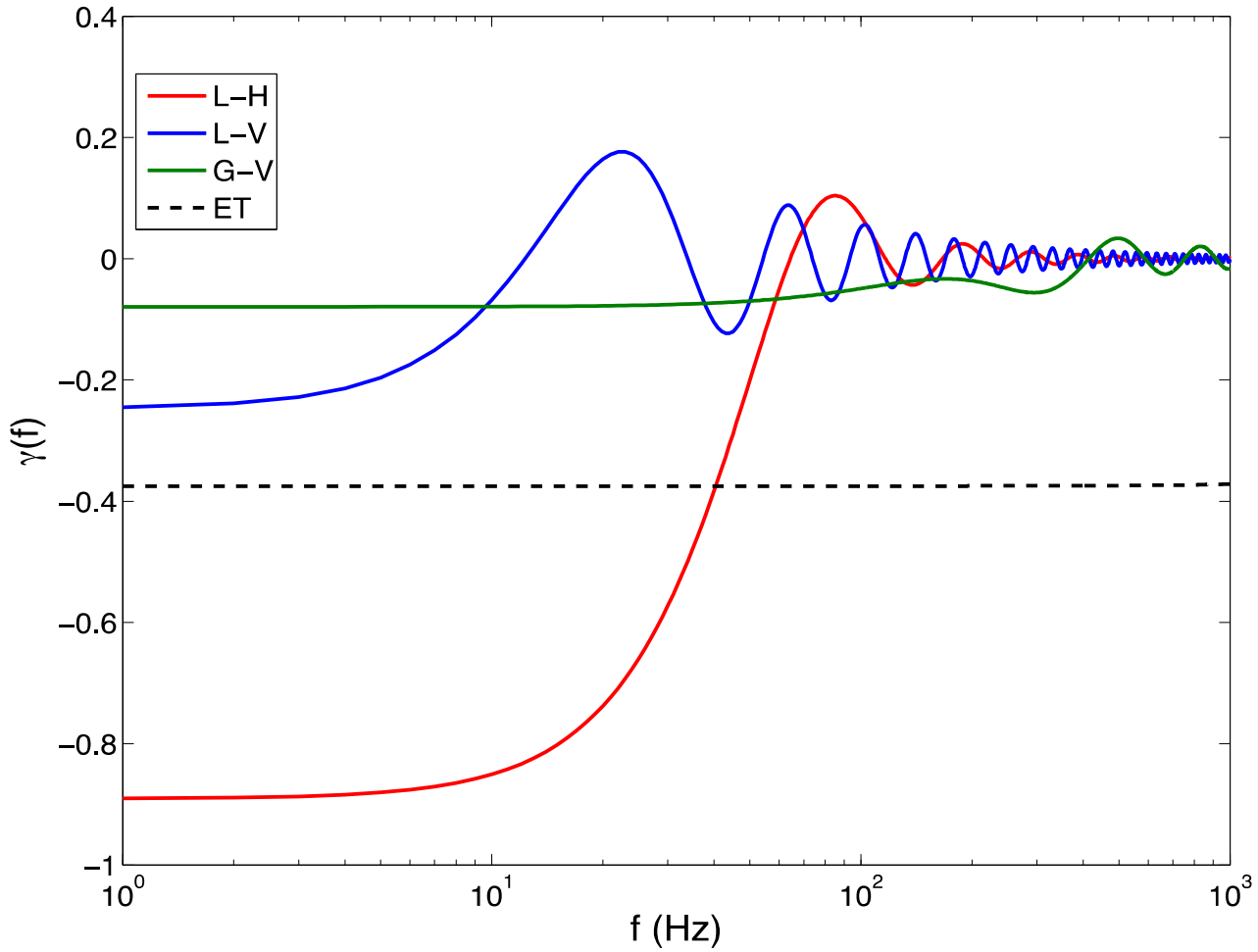

Gravitational Waves and Laser Interferometers

Measurements are made in the presence of noise;

$$x_1(t)=z_1(t)+n_1(t)\ ,\quad x_2(t)=z_2(t)+n_2(t)$$

For example, the shot noise (Poisson statistics) of the laser.

$$h(f)=\frac{1}{4|B(\eta)|}\left[\frac{\hbar}{P}\omega\right]^{1/2}$$

$N_1(f)=\hbar\omega/4P$, where

$$\lim_{T\to\infty}\frac{1}{T}\int_0^T n_1^2(t)dt=\int_0^\infty N_1(f)df$$

Gravitational Waves and Laser Interferometers

$$\frac{S}{N} = \frac{\langle z_1 z_2 \rangle_{\text{av}}}{\left[(1/2T) \int_0^\infty N_1(f) N_2(f) df \right]^{1/2}}$$

The denominator is the variance of the correlation.

The 95% (frequentist) upper limit would be:

$$\langle z_1 z_2 \rangle_{\text{av}} \leq 1.645 \left[\frac{1}{2T} \int_0^\infty N_1(f) N_2(f) df \right]^{1/2}$$

Gravitational Waves and Laser Interferometers

Filter the data. Transfer function of the filter $D(\eta)$.

$$\langle z_1(t) z_1(t+\tau)_{\rm av} = \int_0^\infty \frac{d\eta\, 8G\rho_g(\eta)|B(\eta)|^2|D(\eta)|^2}{c^2\eta^2}\gamma(\mathbf{x}_1,\mathbf{x}_2,\eta,\tau)\ , \tag{4.13}$$

while the variance of this will be

$$\sigma^2 = \left[\frac{1}{2T}\int_0^\infty N_1(f)N_2(f)|D(f)|^4 df\right]^{1/2}\ . \tag{4.14}$$

Gravitational Waves and Laser Interferometers

There is an optimal filter that will maximize the signal-to-noise ration, S/N.

$$|D(f)|^2 = k\frac{\rho_g(f)|B(f)|^2\gamma(\mathbf{x}_1,\mathbf{x}_2,f)}{N_1(f)N_2(f)f^2}$$

$$\frac{S}{N} = \frac{2G}{\pi^2c^2}\left[2T\int^{\infty}\left[\frac{\rho_g(f)|B(f)|^2\gamma(\mathbf{x}_1,\mathbf{x}_2,f)}{f^2}\right]^2\frac{df}{N_1(f)N_2(f)}\right]^{1/2}$$

So in terms of a 95% upper limit (S/N ~ 1.645) on Ω_{gw}

$$\Omega_{gw}(f) = \frac{\pi c^2 f^3}{\rho_c G|\gamma(\mathbf{x}_1,\mathbf{x}_2,f)|}\left[\frac{2}{\Delta f T}\right]^{1/2}(1.645)h_n^2(f)$$

Isotropic search

- Frequency domain cross product:

$$Y = \int \tilde{s}_1^*(f)\tilde{Q}(f)\tilde{s}_2(f)df$$

- optimal filter:

$$\tilde{Q}(f) \propto \frac{\gamma(f)\Omega_{gw}(f)}{f^3 P_1(f)P_2(f)} \text{ with } \Omega_{gw}(f) \equiv \Omega_\alpha f^\alpha$$

- in the limit noise >>GW signal

$$\text{Mean}(Y) = \Omega_0 T,\ \text{Var}(Y) \equiv \sigma^2 \mu T,\ \text{SNR } \mu \sqrt{T}$$

O1 Stochastic Search Results

- No evidence for a stochastic background for both the isotropic and direction searches
- Put upper limits on the energy density for different power indices
- Took a long time to clean the data.
- For α=0, the isotropic bound is 33x better than with initial LIGO/Virgo

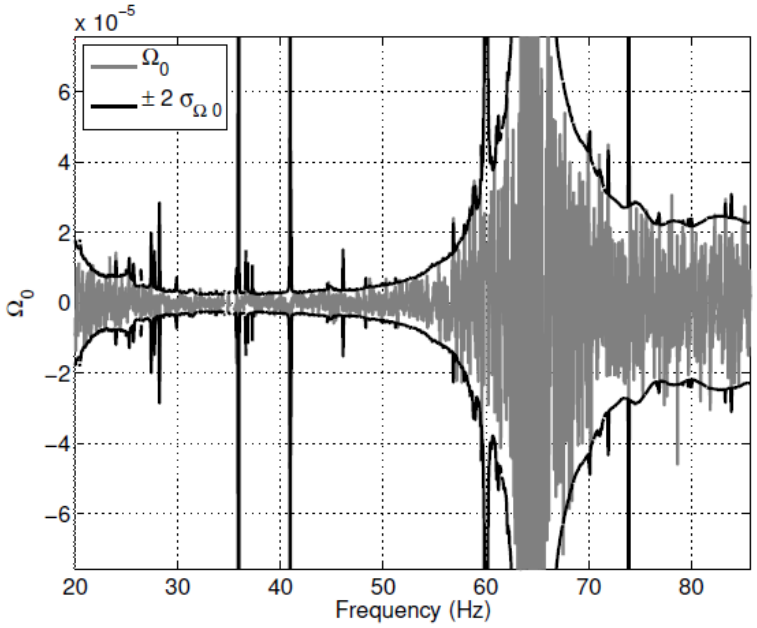

$$\Omega_{gw}(25\text{Hz}) < 1.7 \times 10^{-7}$$

(LSC-Virgo) PRL.118.121101 (2017)

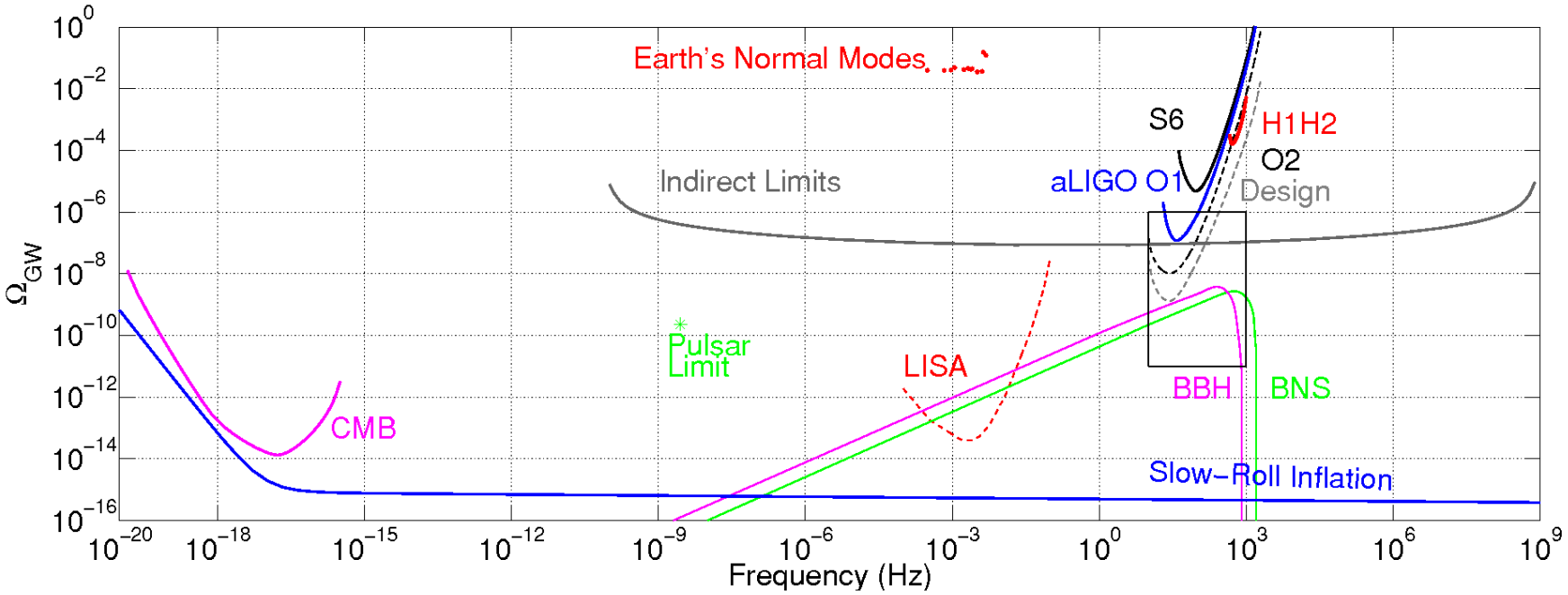

Indirect limits: P. Lasky et al., PhysRevX.6.011035 (2016)
"CMB temperature and polarization power spectra, lensing, BAOs and BBN"

PI integrated sensitivity curves: E. Thrane & J. Romano PhysRevD.88.124032 (2013)
''The LISA sensitivity curve corresponds to an autocorrelation measurement in a single detector assuming perfect subtraction of instrumental noise and/or any unwanted astrophysical foreground."

(LSC-Virgo) PRL.118.121101 (2017)

Spectral index α	Frequency band with 99% sensitivity	Amplitude Ω_α	95% CL upper limit	Previous limits [36]
0	$20 - 85.8$ Hz	$(4.4 \pm 5.9) \times 10^{-8}$	1.7×10^{-7}	5.6×10^{-6}
2/3	$20 - 98.2$ Hz	$(3.5 \pm 4.4) \times 10^{-8}$	1.3×10^{-7}	–
3	$20 - 305$ Hz	$(3.7 \pm 6.5) \times 10^{-9}$	1.7×10^{-8}	7.6×10^{-8}

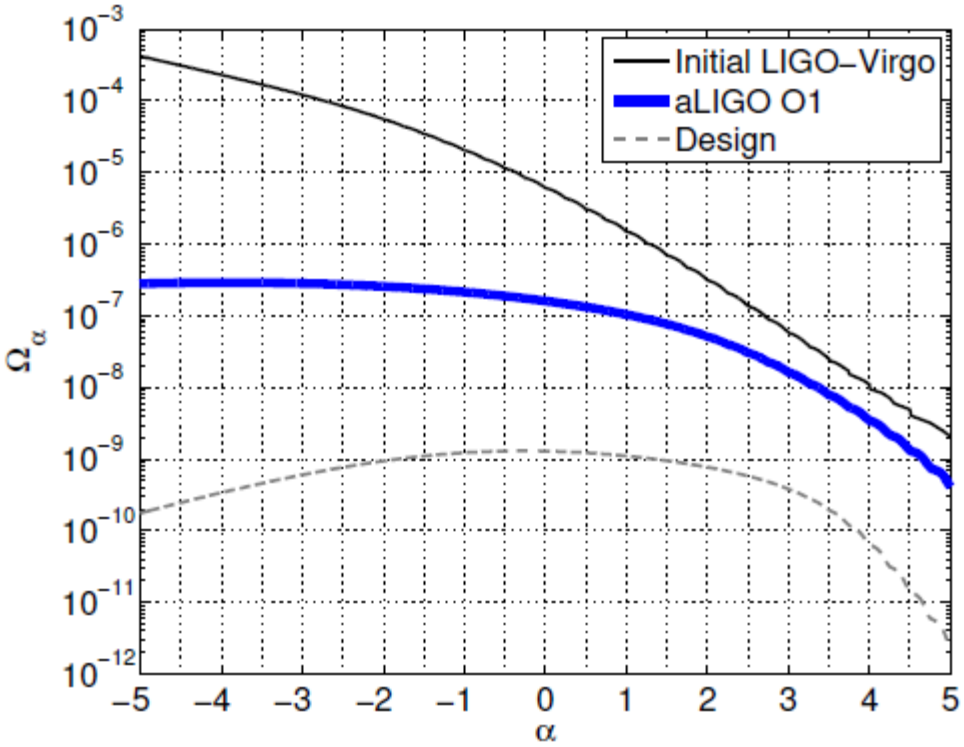

FIG. 2. Following [52], we present 95 % confidence contours in the $\Omega_\alpha - \alpha$ plane. The region above these curves is excluded at 95% confidence. We show the constraints coming from the final science run of Initial LIGO-Virgo [36] and from O1 data. Finally, we display the projected (not observed) design sensitivity to Ω_α and α for Advanced LIGO and Virgo [54].

(LSC-Virgo) PRL.118.121101 (2017)

Directional searches

- Relax assumption of isotropy and generalize the search for a stochastic signal to the case of arbitrary angular distribution.

$$\Omega_{\rm GW}(f) \equiv \frac{f}{\rho_c}\frac{d\rho_{\rm GW}}{df} = \frac{2\pi^2}{3H_0^2} f^3 H(f) \int_{S^2} d\hat{\Omega}\, \mathcal{P}(\hat{\Omega})$$

$$\mathcal{P}(\hat{\Omega}) = \mathcal{P}_\alpha \mathbf{e}_\alpha(\hat{\Omega})$$

Radiometer Analysis

Spherical Harmonic Decomposition

$$\mathcal{P}(\hat{\Omega}) \equiv \eta(\hat{\Omega}_0)\delta^2(\hat{\Omega},\hat{\Omega}_0)$$

$$\mathcal{P}(\hat{\Omega}) \equiv \sum_{lm} \mathcal{P}_{lm} Y_{lm}(\hat{\Omega})$$

O1 Directional – Extended Sources

Spherical Harmonics (SHD)

All-sky (broadband) Results

α	$\Omega_{\rm gw}$	$H(f)$	f_α (Hz)	θ (deg)	$l_{\rm max}$	Max SNR (% p-value) BBR	Max SNR (% p-value) SHD	Upper limit range BBR ($\times 10^{-8}$)	Upper limit range SHD ($\times 10^{-8}$)
0	constant	$\propto f^{-3}$	52.50	55	3	3.32 (7)	2.69 (18)	10 – 56	2.5 – 7.6
2/3	$\propto f^{2/3}$	$\propto f^{-7/3}$	65.75	44	4	3.31 (12)	3.06 (11)	5.1 – 33	2.0 – 5.9
3	$\propto f^{3}$	constant	256.50	11	16	3.43 (47)	3.86 (11)	0.1 – 0.9	0.4 – 2.8

SNR maps

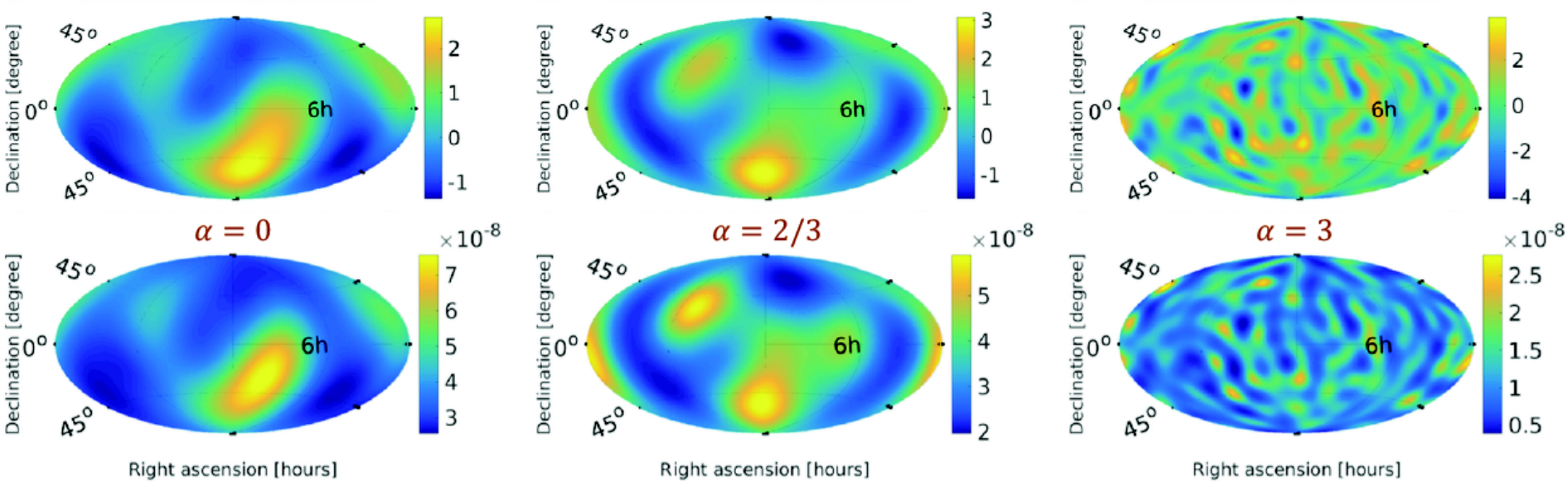

Upper Limit maps [$\Omega_{\rm gw}$ sr^{-1}]

(LSC-Virgo)
PRL.118.121102 (2017)

O1 Directional – Point Sources

Broadband Radiometer (BBR)

All-sky (broadband) Results

						Max SNR (% p-value)		Upper limit range	
α	$\Omega_{\rm gw}$	$H(f)$	f_α (Hz)	θ (deg)	$l_{\rm max}$	BBR	SHD	BBR ($\times 10^{-8}$)	SHD ($\times 10^{-8}$)
0	constant	$\propto f^{-3}$	52.50	55	3	3.32 (7)	2.69 (18)	$10-56$	$2.5-7.6$
2/3	$\propto f^{2/3}$	$\propto f^{-7/3}$	65.75	44	4	3.31 (12)	3.06 (11)	$5.1-33$	$2.0-5.9$
3	$\propto f^{3}$	constant	256.50	11	16	3.43 (47)	3.86 (11)	$0.1-0.9$	$0.4-2.8$

SNR maps

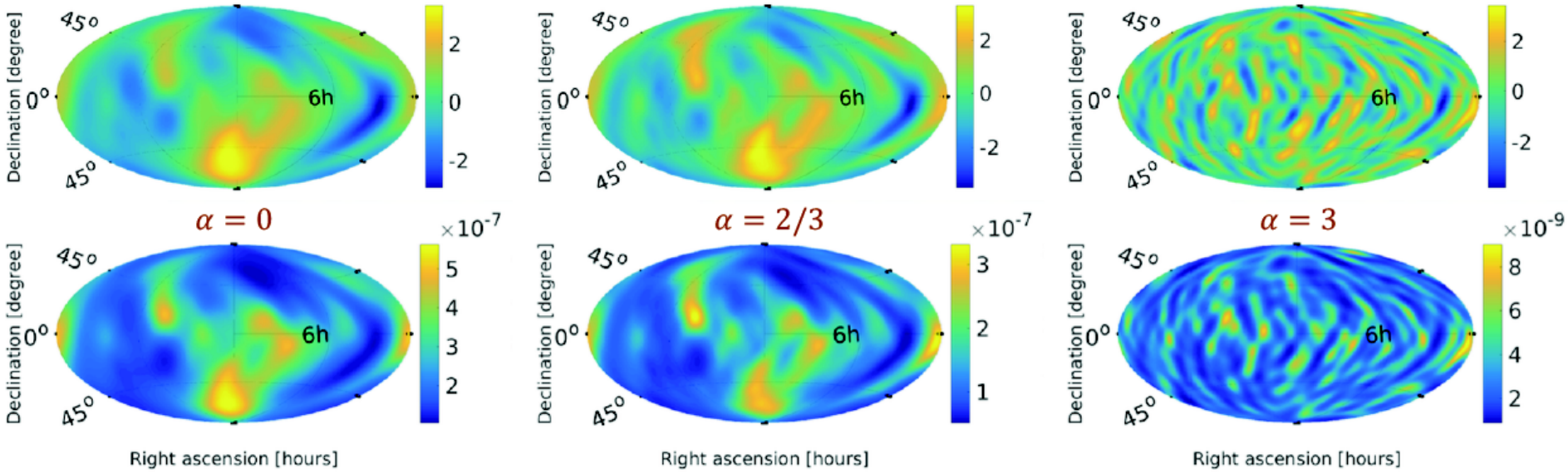

Upper Limit maps [erg cm^{-2} s^{-2} Hz^{-1}]

(LSC-Virgo)
PRL.118.121102 (2017)

O1 Directional – Directed

Narrowband radiometer

Results showing 90% upper limits on strain as a function of frequency for O1

Sco X-1

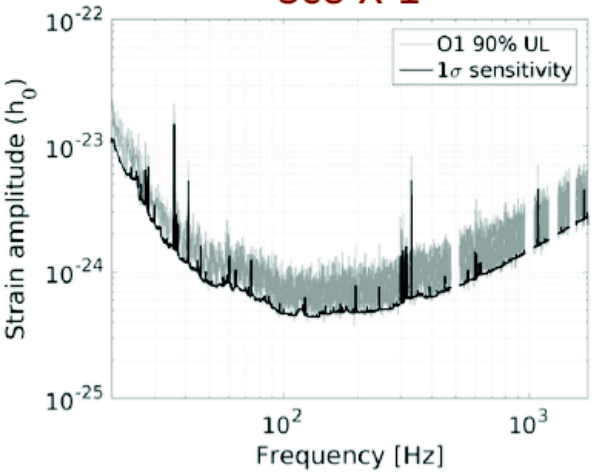

Galactic Centre

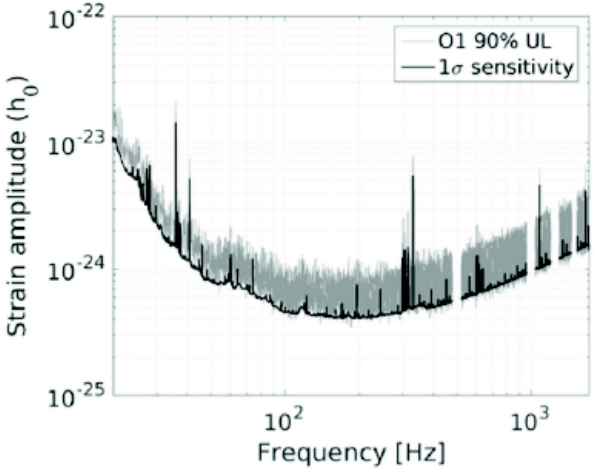

SN1987A

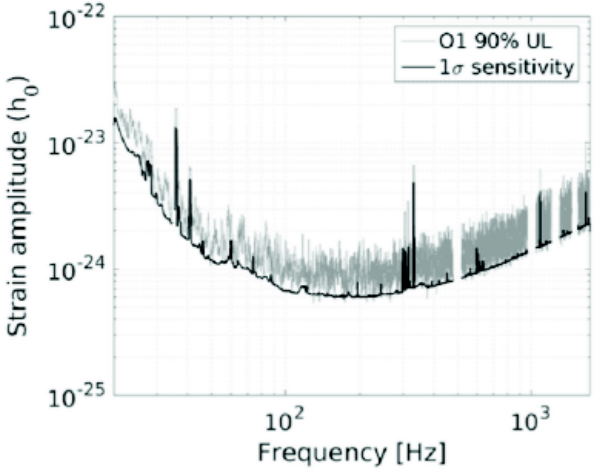

Narrowband Radiometer Results

Direction	Max SNR	p-value (%)	Frequency band (Hz)	Best UL ($\times 10^{-25}$)	Frequency band (Hz)
Sco X-1	4.58	10	616 – 617	6.7	134 – 135
SN1987A	4.07	63	195 – 196	5.5	172 – 173
Galactic Center	3.92	87	1347 – 1348	7.0	172 – 173

PRL.118.121102 (2017)

O1 Binary Black Hole Events

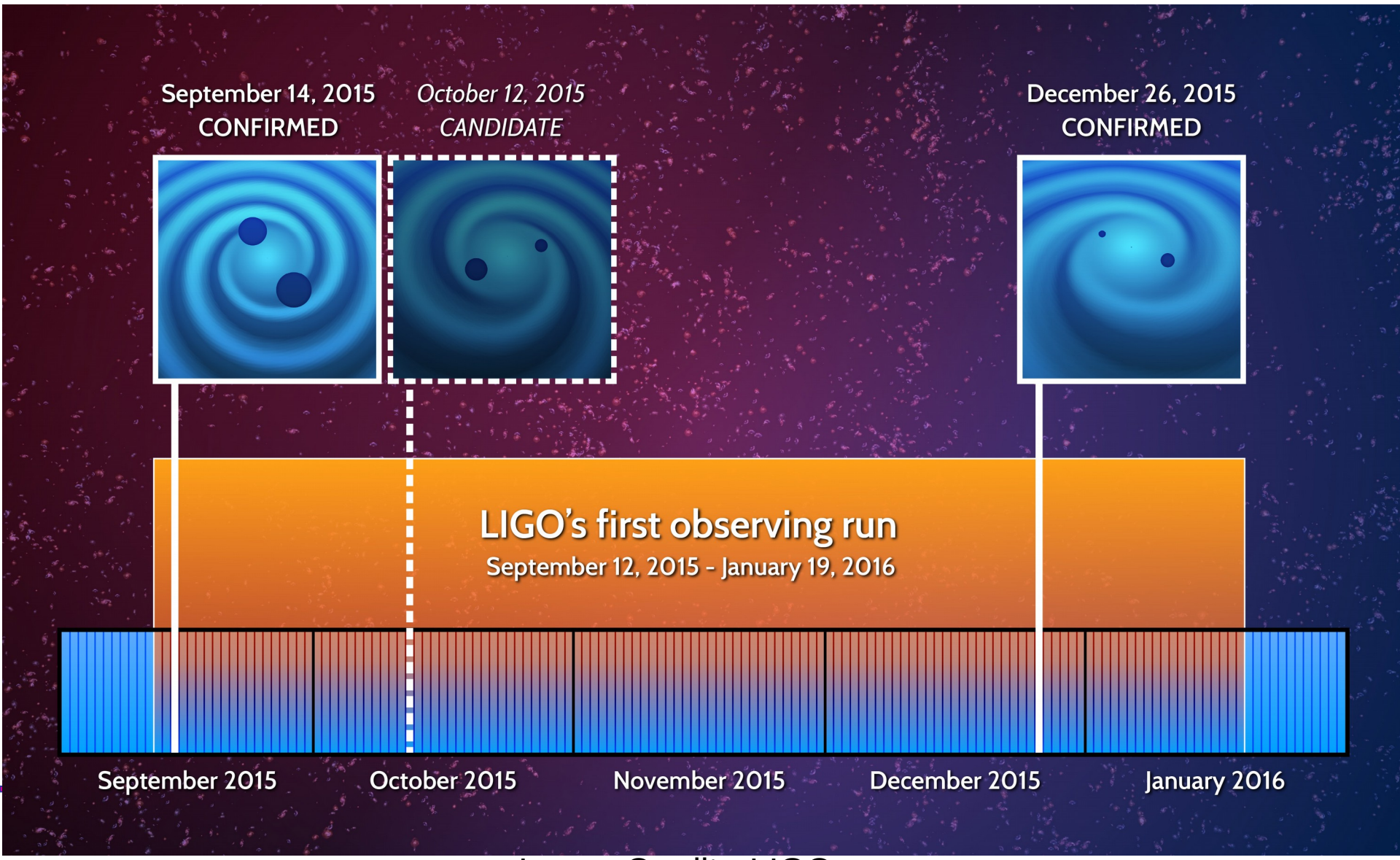

Image Credit - LIGO

Implications of LIGO first detections

- On Sept 14th 2015 LIGO detected for the first time the GW signal from a stellar binary black hole (BBH) at z~0.1 (GW150914). *PhysRevLetter.116.061102*
- Another event (GW151226), and likely a third (LVT151012), were detected in the LIGO first observational run. *PRX 6, 041015 (2016).*
- Besides the detection of loud individual sources at close distances, we expect to see the background formed by all the sources from the whole Universe (up to z~20)
- GW150914 told us that black hole masses ($m_{1,2}$~$30M_o$) can be larger than previously expected.
- Revised previous predictions of the GW background from BBHs, assuming various formation scenarios. *PhysRevLetter.116.131102*

Binary Black Hole Merger Rate

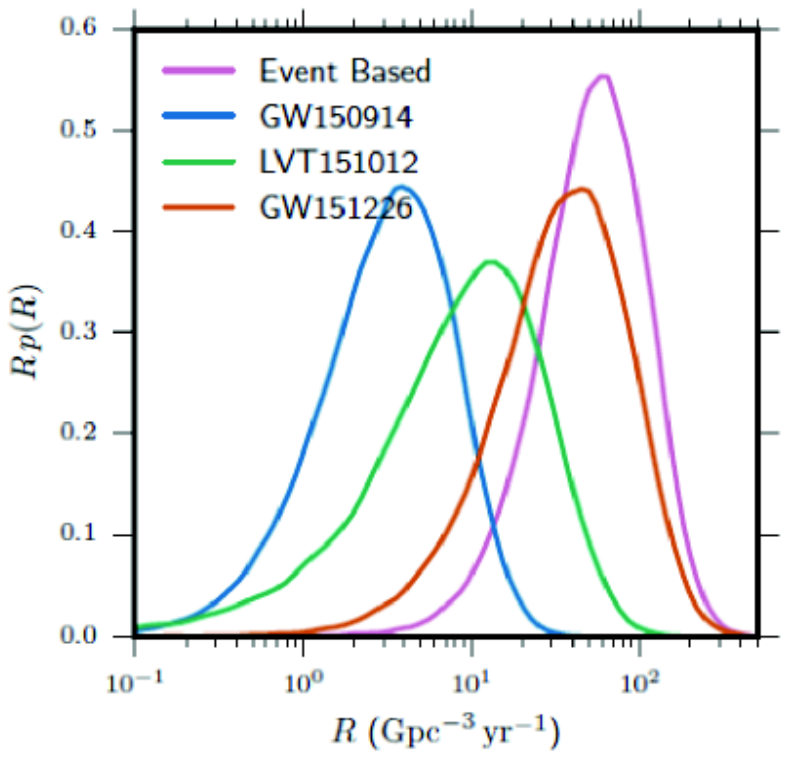

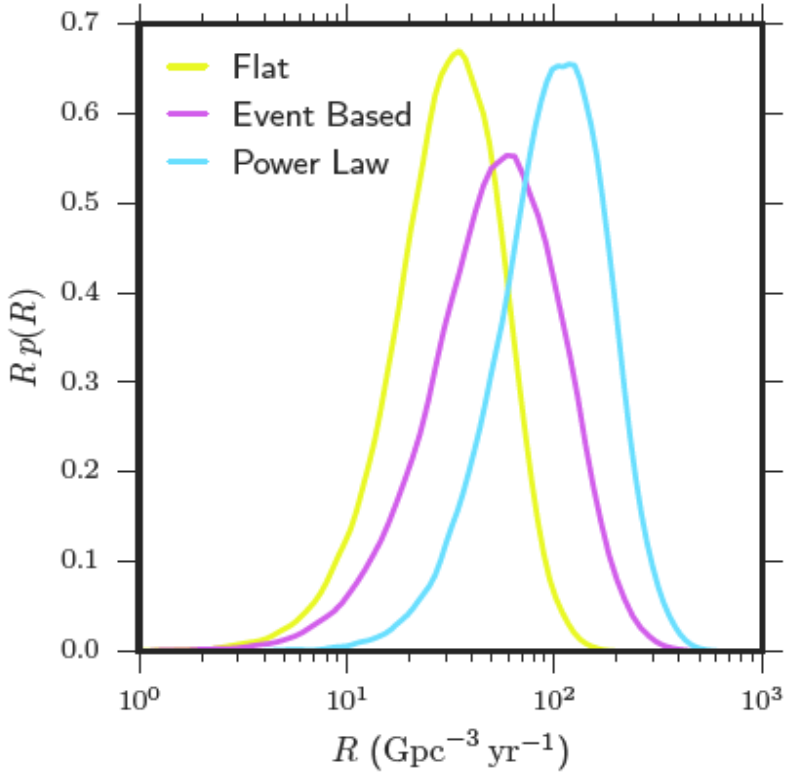

90% allowed range: [9-240] /Gpc^3/yr

PHYSICAL REVIEW X 6,041015 (2016)

Astrophysics: Binary Formation

- Two binary formation mechanisms have been proposed.
- Field:
  - » Starting from a binary star system, with each star going through the core-collapse to a black hole.

- Dynamic:
  - » Individually formed black holes in dense environments (globular clusters) fall toward the center of the potential well, where they dynamically form binaries (and are often ejected).

Implications for a Stochastic Background of GWs

- For every detected binary merger, there are many more that are too distant and too faint.

- They generate a stochastic background of gravitational waves.

Merger Rate

Source Energy Spectrum

$$\Omega_{\rm GW}(f;\theta_k) = \frac{f}{\rho_c H_0}\int_0^{z_{\rm max}} dz \frac{R_m(z,\theta_k)\frac{dE_{\rm GW}}{df_s}(f_s,\theta_k)}{(1+z)E(\Omega_{\rm M},\Omega_\Lambda,z)}$$

Cosmology

- Relatively high rate and large masses of observed systems implies a relatively strong stochastic background.

Implications for a Stochastic Background of GWs

Probing compact binary decays predominantly between z ~ 1 – 3.

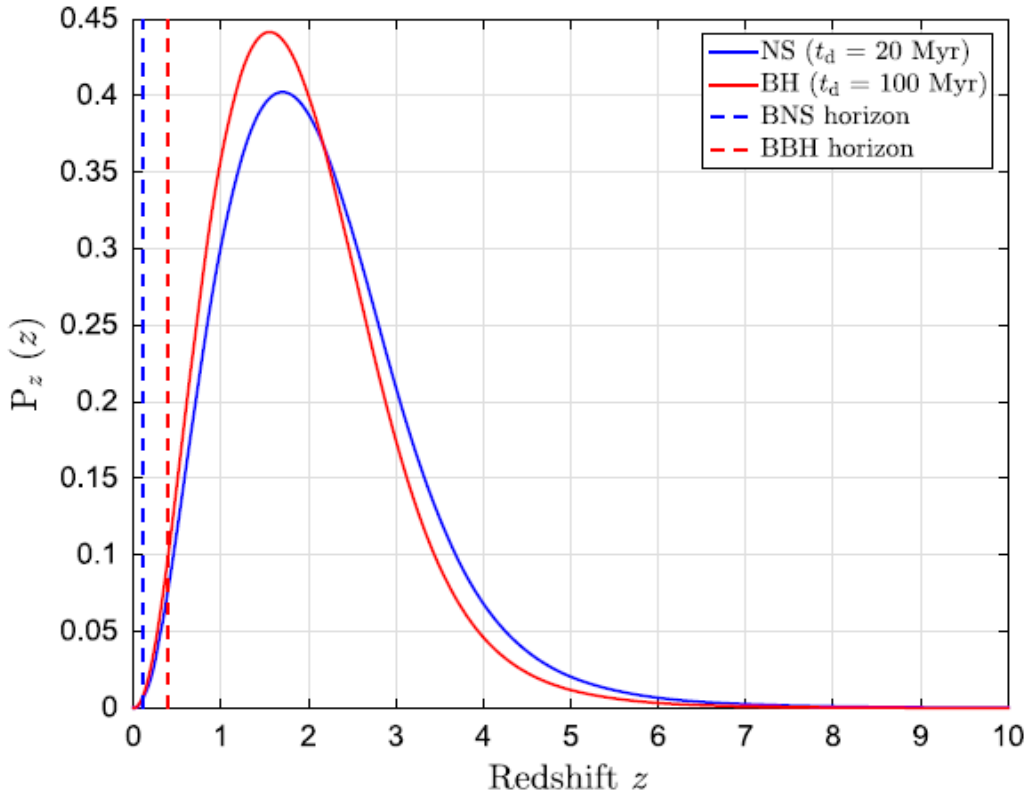

Source redshift probability distribution for binary neutron stars and (blue) and binary black holes (red).

PHYSICAL REVIEW D 92,063002 (2015)

Implications for a Stochastic Background of GWs

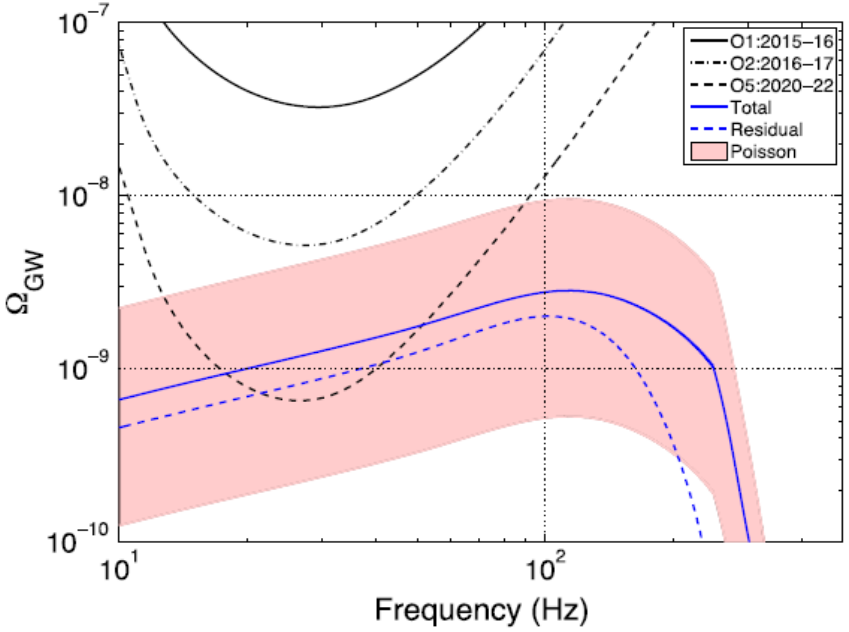

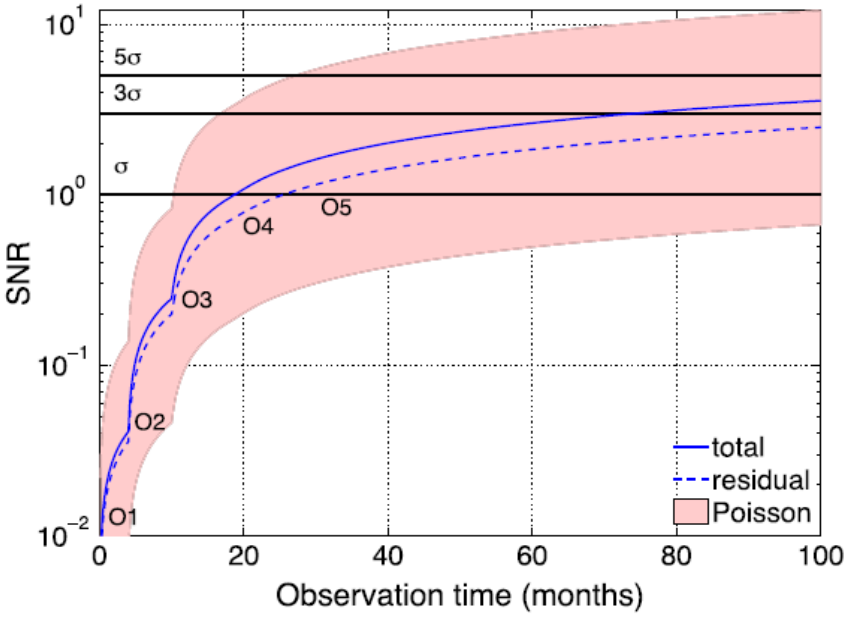

Based on the Field formation mechanism, assuming GW150914 parameters.

Assumptions are necessary; best information available in literature.

Abbott et all (LIGO-Virgo) Physical Review Letters **116**, 131102 (2016)

Alternative Models

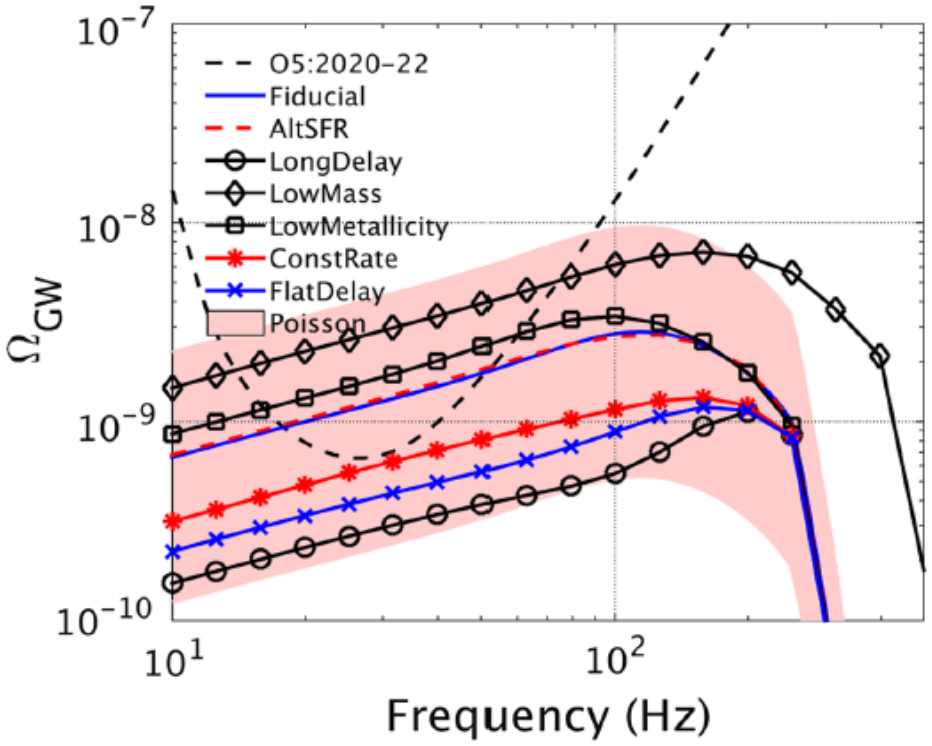

- Model variations imply relatively small changes in the energy spectrum.
- Large Poisson statistical uncertainty.
- Dominated by z ~1-2 contributions.
- Conservative estimates.
- A foreground to cosmological models of stochastic background.

Abbott et all (LIGO-Virgo) Physical Review Letters **116**, 131102 (2016)

Implications for a Stochastic Background of GWs

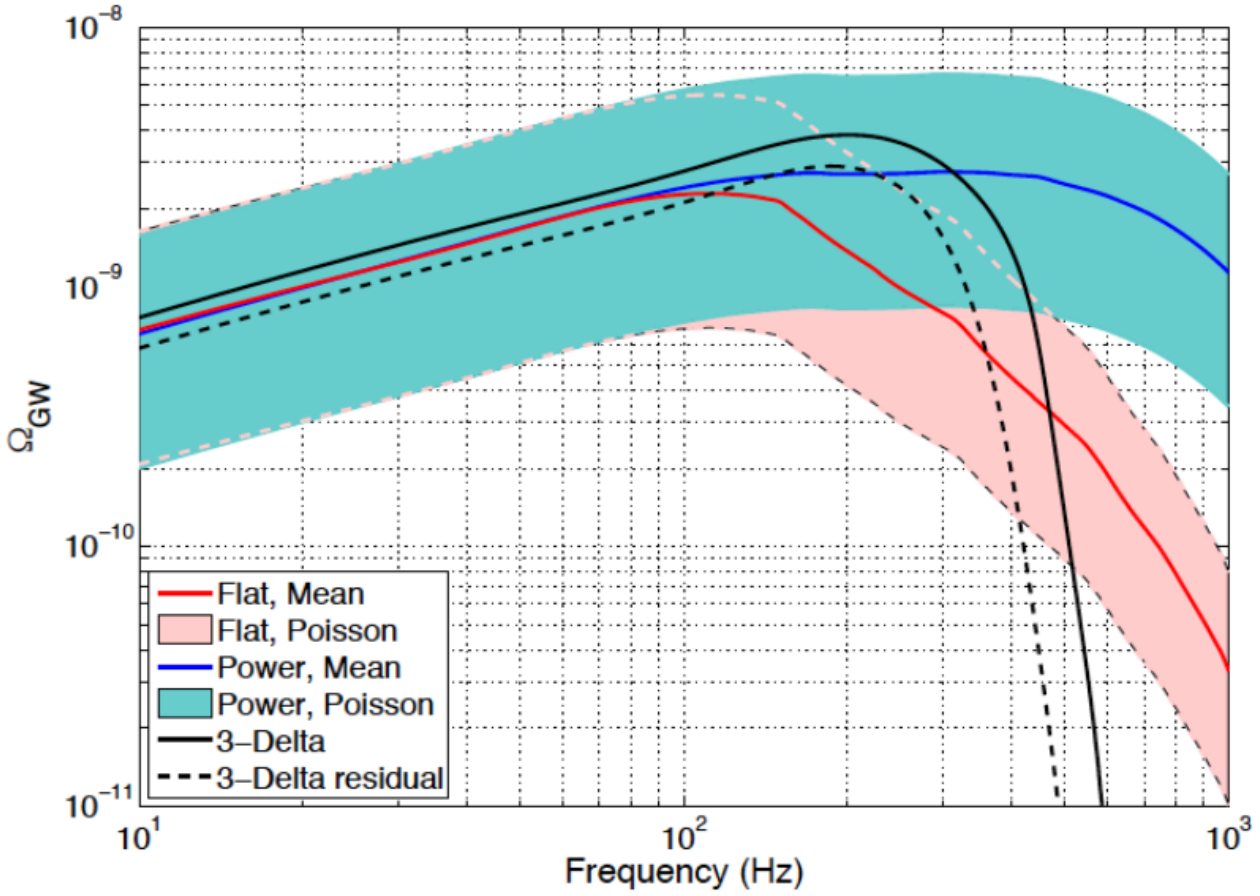

All of O1.

3 events.

Same mean value Ω_{gw} (25 Hz)~ 10^{-9}

Less uncertainty

Abbott et all (LIGO-Virgo), Phys. Rev. X 6, 041015 (2016)

There is a good chance that LIGO-Virgo will observe this BBH produced stochastic background in the next 3 to 5 years.

Gravitational wave background from Population III binary black holes consistent with cosmic reionization

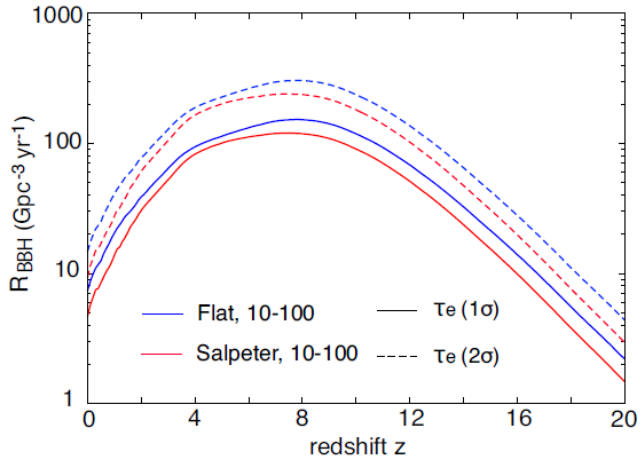

Figure 3. Merger rate of PopIII BBHs for different assumed IMFs, as in Fig. 2. The data is taken from K14, but renormalized to be consistent with the electrons scattering optical depth τ_e measured by *Planck* within the 1σ (solid) and 2σ (dashed) error (Eq. 1 with $f_{\rm esc,m} = 0.1$ and $\eta_{\rm ion} = 5 \times 10^4$).

Potentially a stronger stochastic background than what we would expect from direct BBH observations.

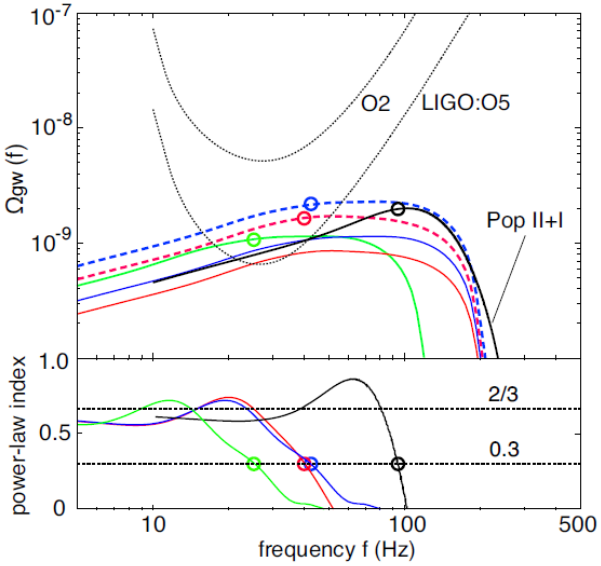

Figure 4. *Top*: spectra of GWB produced by PopIII BBHs for the same IMFs, $f_{\rm esc,m}$ and $\tau_{\rm e}$ as in Fig. 3 (blue and red curves). We assume binaries with the average chirp mass of $\langle M_{\rm chirp} \rangle = 30\ {\rm M}_\odot$ on circular orbits. The background expected from all unresolved PopII+PopI BBHs is shown for reference (solid black curve, Abbott et al. 2016b, their fiducial model). Black dotted curves show the expected sensitivity of AdLIGO/Virgo in the observing runs O2 and O5. The green solid curve is the same as the blue solid curve, but with a higher chirp mass of $\langle M_{\rm chirp} \rangle = 50\ {\rm M}_\odot$ and with a lower merging rate by a factor of 3/5. *Bottom*: the spectral index; open circles mark the frequencies above which $\alpha < 0.3$.

K. Inayoshi et al., Mon Not R Astron Soc (2016) 461 (3): 2722-2727.

Did LIGO Detect Dark Matter?

- "There remains a window for masses 20 $M_{\odot} \lesssim M_{bh} \lesssim 100\ M_{\odot}$ where primordial black holes (PBHs) may constitute the dark matter."
- Reasonable rate estimates overlap LIGO rate limits.
- No neutrino or optical counterparts.
- "They may be distinguished from mergers of BHs from more traditional astrophysical sources through the observed mass spectrum, their high ellipticities, or their stochastic gravitational wave background." S. Bird et al., PRL 116, 201301 (2016)
- "We show that if PBHs make up the dark matter, then roughly one event should have a detectable eccentricity given LIGO's expected sensitivity and observing time of six years." I. Cholis et al., PRD 94, 084013 (2016)

Stochastic Background – Primordial Black Hole

"We have shown that the amplitude of this spectrum is significantly lower than that arising from the stellar BBH mergers, although there is currently a large uncertainty in the local merger rate for stellar BBH systems.

...

Consequently, the stochastic GW background measurement with Advanced LIGO detectors is unlikely to detect this background."

Other studies are more optimistic:

https://arxiv.org/abs/1610.08725
https://arxiv.org/abs/1610.08479

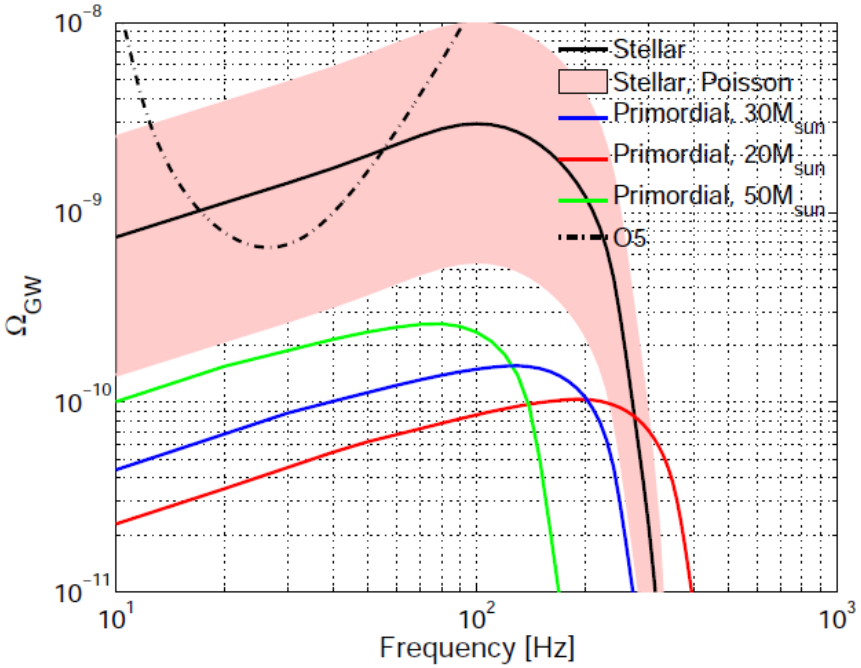

FIG. 4: Gravitational-wave energy density for the primordial BBH model is shown as a function of frequency for several values of the black hole mass, assuming the Ludlow et al. concentration model [28] and the Watson et al. model of the halo mass function [31]. Also shown is the projected final sensitivity of advanced detectors, denoted O5, as well as the fiducial stellar model and its Poisson error band [34].

V. Mandic et al., Phys. Rev. Lett. **117**, 201102 (2016)

Correlated Magnetic Noise from the Schumann Resonances

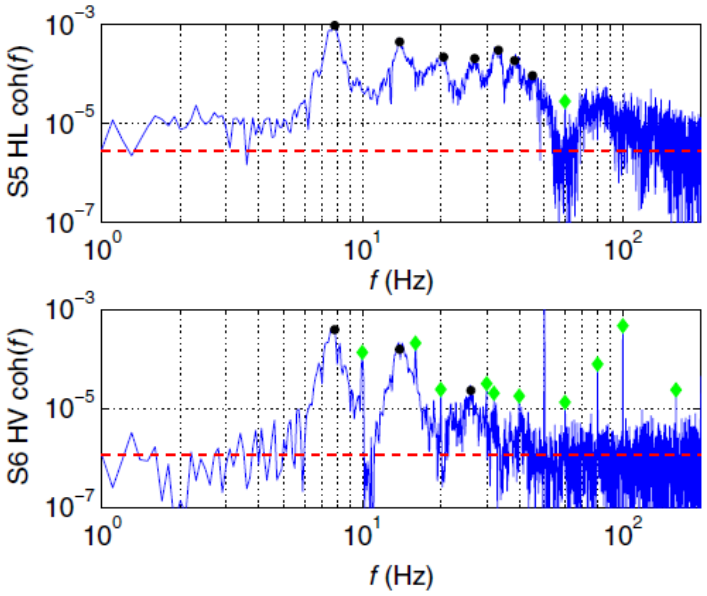

FIG. 1 (color online). Magnetometer coherence spectra for LHO-LLO during the LIGO S5 science run (top, t_{obs} = 330 dy) and for LHO-Virgo during S6-VSR2/3 (bottom, t_{obs} = 100 dy). Schumann resonance peaks are indicated with black circles while electronic noise lines are indicated with green diamonds. The red dashed line indicates the average value expected for uncorrelated noise. Some LHO-LLO peaks are obscured by 60 Hz electronic noise. The frequency resolution is 0.1 Hz.

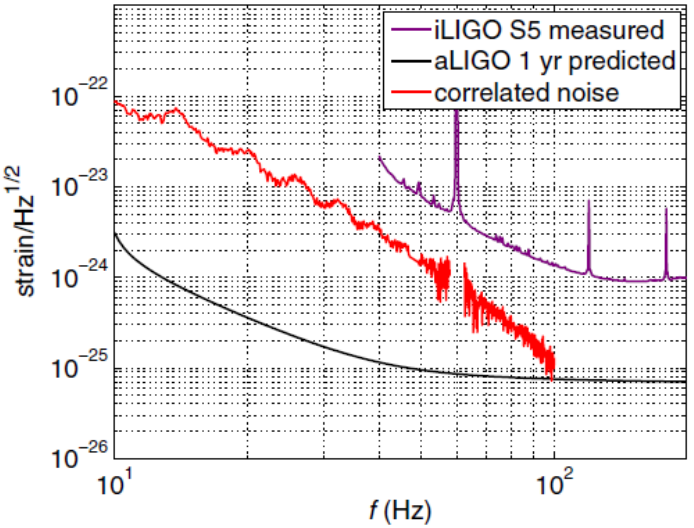

FIG. 3 (color online). Strain amplitude spectra for correlated and uncorrelated noise. Black is the uncorrelated noise $\sqrt{N^{u}_{12}(f)}$ for the H1L1 detector pair operating at Advanced LIGO design sensitivity and assuming 1 yr of integration. Purple indicates the uncorrelated noise $\sqrt{N^{u}_{12}(f)}$ achieved during initial LIGO using ≈300 days of coincident data. Red is $\sqrt{N^{m}_{12}(f)}$ (the estimated correlated noise due to EM fields during initial LIGO). Electronic noise lines have been notched. The spectra have been scaled to assume a frequency resolution of 0.25 Hz, which is typical for stochastic searches [26].

Monitor correlated magnetic noise level in O1 and future runs. E. Thrane et al., PRD **87**, 123009 (2013)

Magnetometer Coherence Virgo - KAGRA

Fun Fact: The Schumann signal is actually a bit stronger underground than above ground at KAGRA.

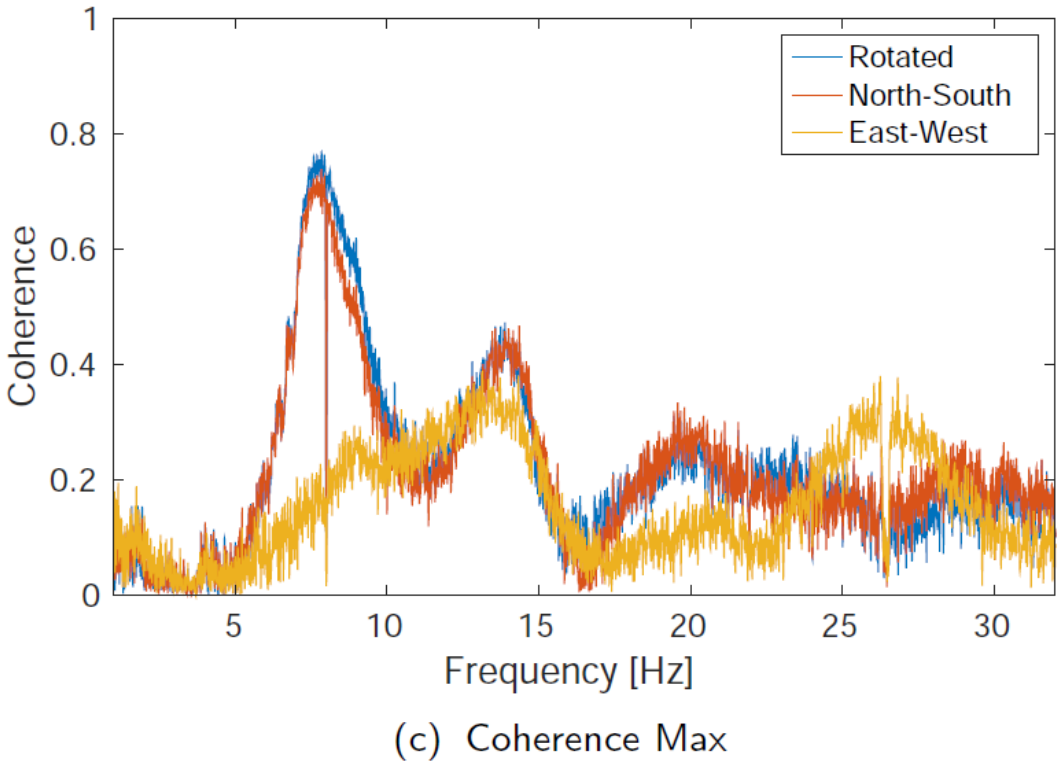

(c) Coherence Max

There is the possibility that the global magnetic fields could limit the ability of LIGO-Virgo-KAGRA to limit or measure the stochastic background.

Wiener Filtering – Low noise magnetometers at the sites.
Studies on-going with many researchers from LIGO, Virgo and KAGRA.

Correlated Transient Magnetic Noise – The Source of the Schumann Resonances

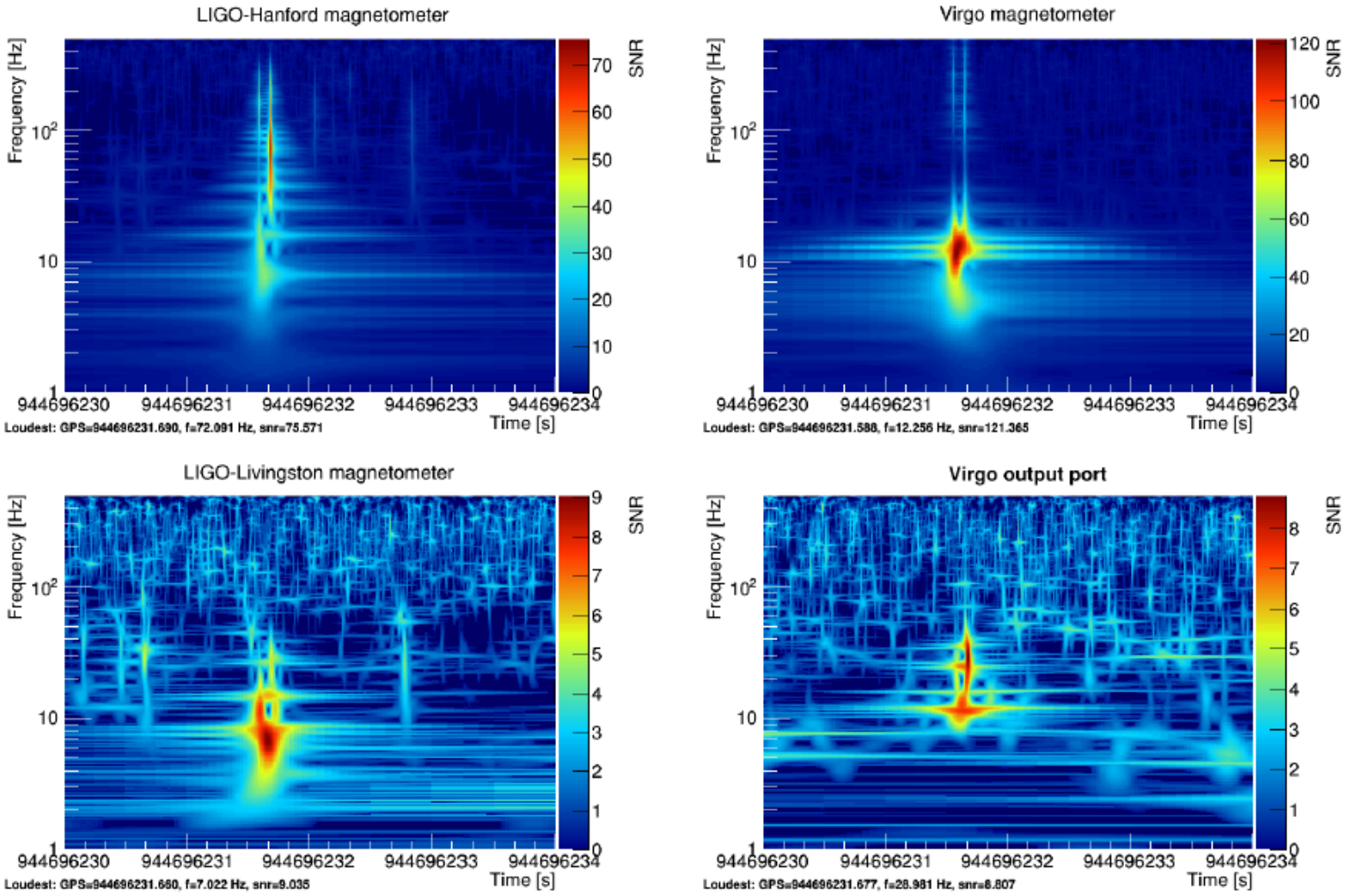

Time-frequency spectrograms of magnetometers located at the LIGO-Hanford, Virgo and LIGO-Livingston at the time of the December 12, 2009 positive Gigantic Jet at 23:36:56.55 UTC. The signal is clearly present in the magnetometers. Bottom right spectrogram shows the event in the Virgo gravitational-wave strain, h(t), data.

Correlated Transient Magnetic Noise – Time Slide Study For Coincident Events

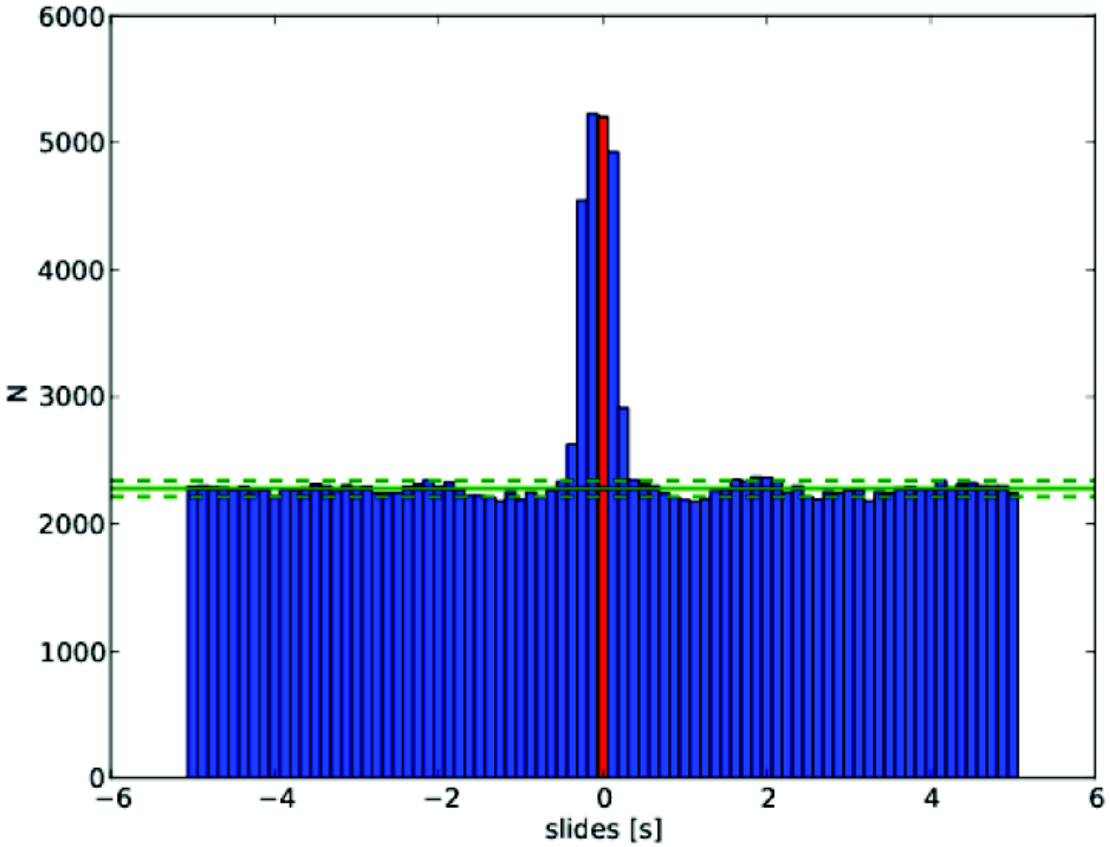

The number of coincident triggers as a function of time delay for magnetometers located at LIGO-Hanford and Virgo. The horizontal line represents the mean value of the time slide results (excluding the 0.625 s covered by the central 5 bins), while the dashed lines represent the standard deviation (again excluding the central 5 bins).

I. Kowalska et al., Classical and Quantum Gravity, Vol. 34, 074002 (2017)

Correlated Transient Magnetic Noise – The Source of the Schumann Resonances

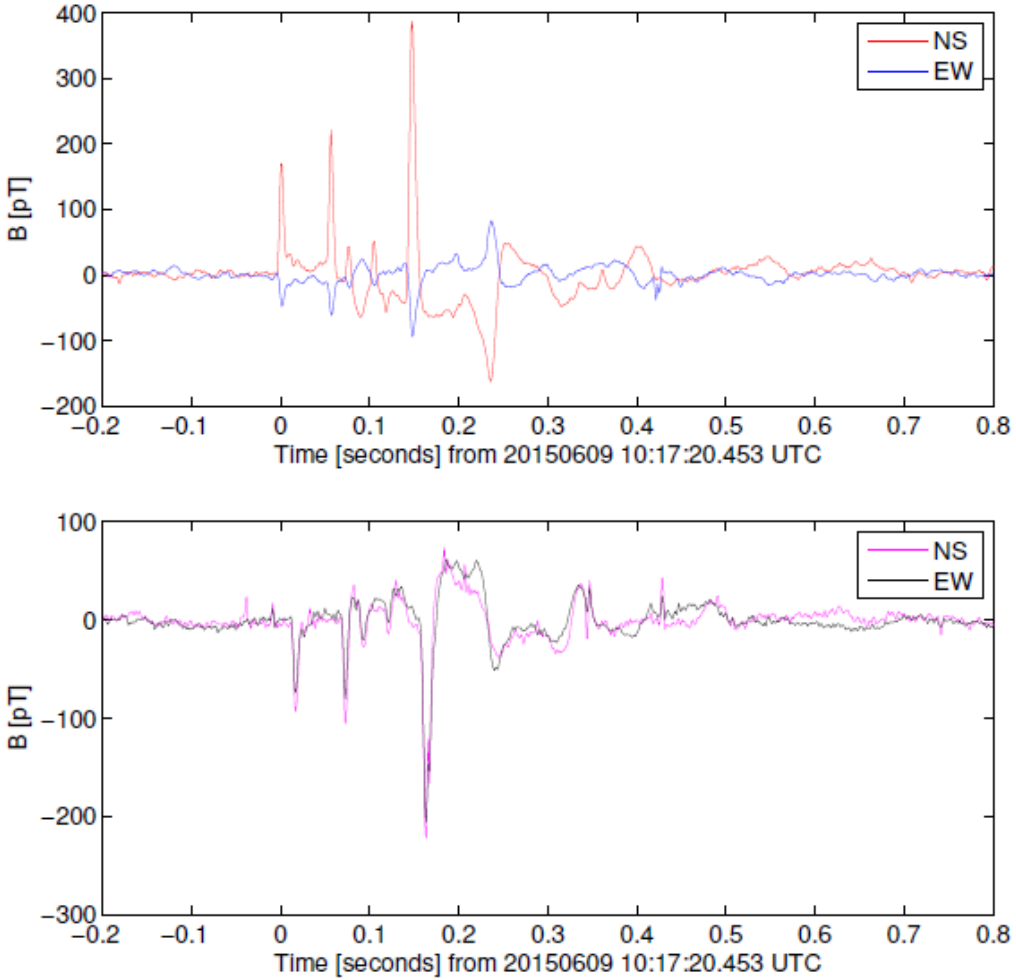

Example: lightning strike in China. 149 kA.

Observed in Poland (top) and Colorado (bottom).

50 to 100 large lightning strikes per second around the Earth.

2 to 3 coincident events per day with B > 200 pT

O1 analysis – verified that Schumann background did not contaminate results.

I. Kowalska et al., Classical and Quantum Gravity, Vol. 34, 074002 (2017)

Constraints on Cosmic String Parameters Coming from O1 Stochastic and Burst Search Results

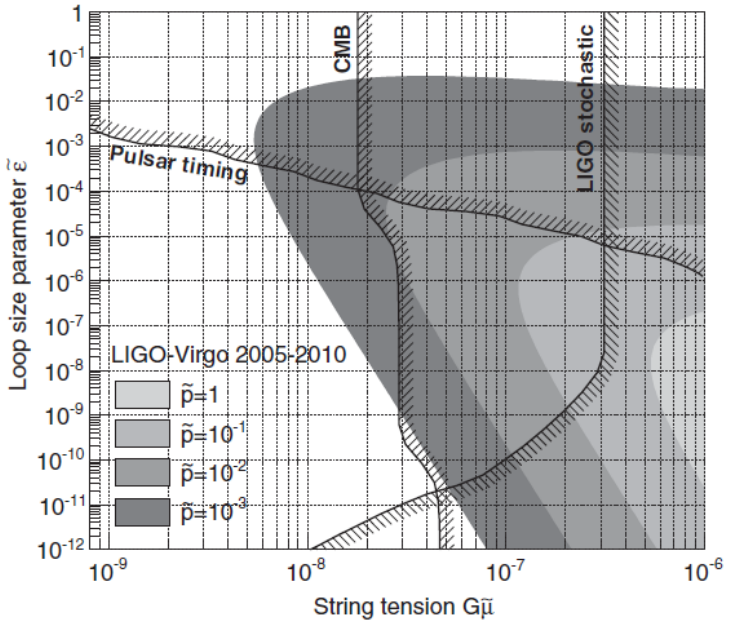

FIG. 2. Constraints on the modified cosmic string parameters $G\tilde{\mu} = g_1 g_2^{-2/3} G\mu$, $\tilde{\varepsilon} = g_1^{-1} g_2^{5/3} \varepsilon$, and $\tilde{p} = (n_c g_1)^{-1} g_2^{-1/3} p$, where g_1, g_2 and n_c are numerical factors of $\mathcal{O}(1)$. The gray regions, in different shades for four reconnection probability values, are rejected by our analysis at a 90% level. The black lines show the bounds derived from the GW stochastic background spectrum for $\tilde{p} = 10^{-3}$ and for a small loop scenario (CMB, pulsar, and LIGO data). The rejected region is always on the right-hand side of these lines.

Initial LIGO-Virgo results, PRL **112**, 131101 (2014)

Test of General Relativity with the Stochastic Gravitational-wave Background

A new search. Using Advanced LIGO O1 (and future) data to search for 6 polarizations. Non-GR. New search pipeline. Theoretical work on-going in parallel.

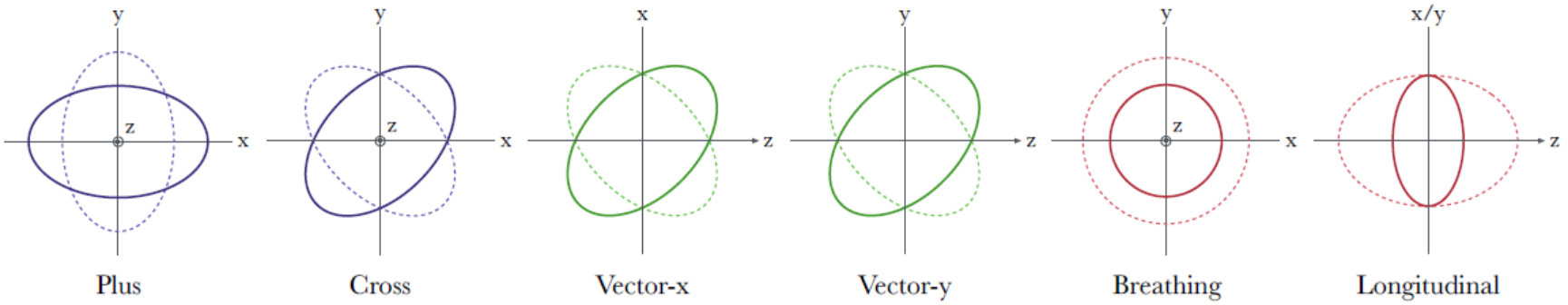

FIG. 1. Deformation of a ring of test particles under the six gravitational wave polarizations allowed in general metric theories of gravity. Each wave is assumed to propagate in the z-direction. While General Relativity allows only for two tensor polarizations (Plus and Cross), alternate theories allow for two vector (X and Y) and/or two scalar (Breathing and Longitudinal) polarization modes.

T. Callister, et al., arXiv:1704.08373

Test of General Relativity with the Stochastic Gravitational-wave Background

To come: results for a search for scalar, vector and tensort polarizations with O1 data.

A fully Bayesian (nested sampling) parameter estimation method will assign upper limits for energy of the different polarizations. Constraints will be placed on various non-GR theories.

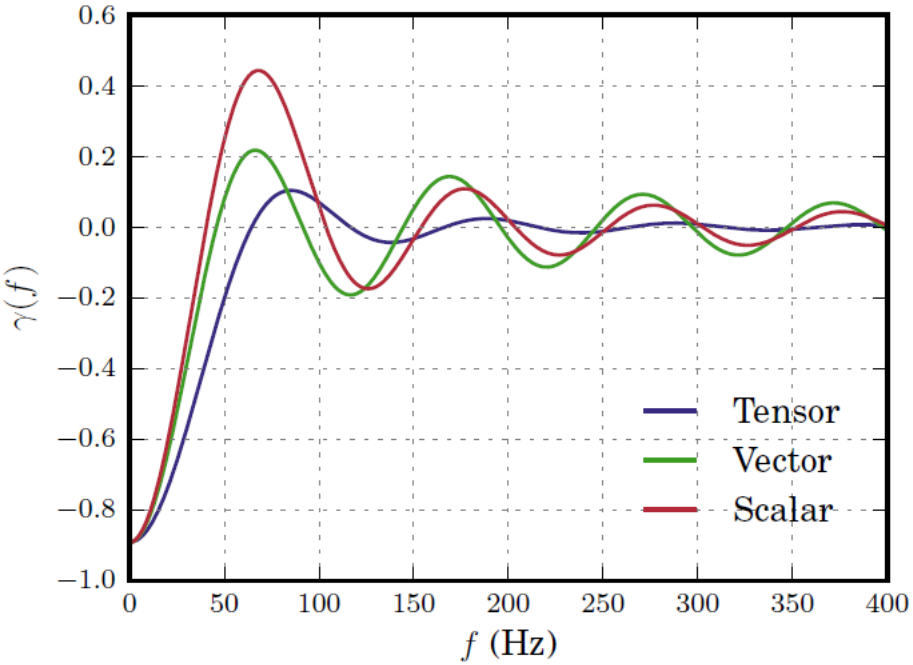

FIG. 2. Overlap reduction functions quantifying Advanced LIGO's sensitivity to isotropic backgrounds of tensor, vector, and scalar-polarized gravitational wave backgrounds.

arXiv:1704.08373

Test of General Relativity with the Stochastic Gravitational-wave Background

Projected sensitivity of Advanced LIGO to SGWBs of tensor, vector, and scalar radiation (solid blue, green, and red, respectively).

The limits that Advanced LIGO can place on flat vector and scalar-polarized backgrounds will therefore be similar to those placed on a flat tensorial background.

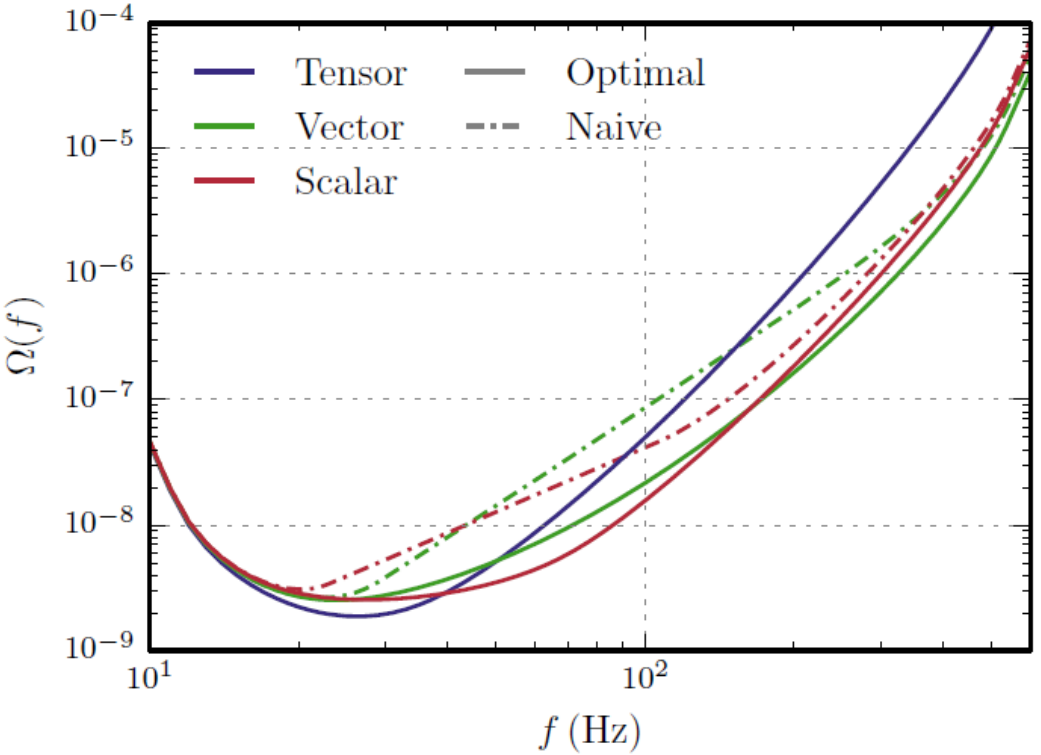

Advanced LIGO can place constraints on positively-sloped vector and scalar backgrounds that are up to an order of magnitude more stringent than those that can be placed on similarly-shaped tensor backgrounds.

Ability to resolve different polarizations will get better with Virgo, KAGRA,LIGO-India.

arXiv:1704.08373

O2 Stochastic Update

- O2 sensitivity comparable to O1
- Many (but not all) noise lines have been cleaned up via commissioning
- O2 will probably have more that 2-times the O1 H1-L1 data
- Combined O1-O2 analysis, you can do the math: $\Omega_{GW} \propto 1/\sqrt{T}$
- Inclusion of Virgo in O2 not likely to change isotropic limit, but could have important implications for the directional searches.
- With Virgo, three detector combinations, and improved sky resolution.

Future Observing Runs

Living Rev. Relativity, **19**, (2016), 1
DOI 10.1007/lrr-2016-1

LIVING REVIEWS in relativity

Prospects for Observing and Localizing Gravitational-Wave Transients with Advanced LIGO and Advanced Virgo

Abbott, B. P. et al.
The LIGO Scientific Collaboration and the Virgo Collaboration
(The full author list and affiliations are given at the end of paper.)
email: lsc-spokesperson@ligo.org, virgo-spokesperson@ego-gw.it

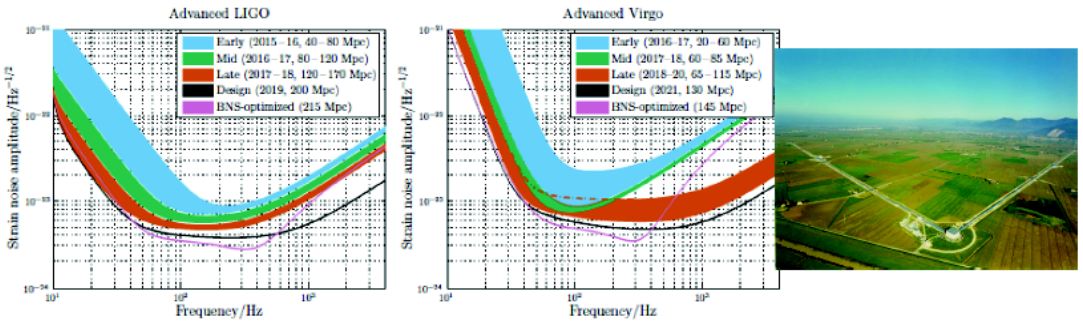

Figure 1: aLIGO (*left*) and AdV (*right*) target strain sensitivity as a function of frequency. The binary neutron-star (BNS) range, the average distance to which these signals could be detected, is given in megaparsec. Current notions of the progression of sensitivity are given for early, mid and late commissioning phases, as well as the final design sensitivity target and the BNS-optimized sensitivity. While both dates and sensitivity curves are subject to change, the overall progression represents our best current estimates.

2015–2016 (O1) A four-month run (beginning 18 September 2015 and ending 12 January 2016) with the two-detector H1L1 network at early aLIGO sensitivity (40–80 Mpc BNS range).

2016–2017 (O2) A six-month run with H1L1 at 80–120 Mpc and V1 at 20–60 Mpc.

2017–2018 (O3) A nine-month run with H1L1 at 120–170 Mpc and V1 at 60–85 Mpc.

2019+ Three-detector network with H1L1 at full sensitivity of 200 Mpc and V1 at 65–115 Mpc.

Living Reviews in Relativity **19**, 1 (2016)

LIGO Observing Run O2 ongoing

LIGO-Virgo Summary/Conclusion

- The GW stochastic background from BBHs is expected to be in the higher end of previous predictions
- The background may be measured by LIGO/Virgo operating at or near design sensitivity.
- No evidence for a stochastic background in O1.
- Upper limit on a flat spectrum 33x better than with initial LIGO/Virgo
- O1 and O2 data will be analyzed together → more observation time

Pulsar Timing

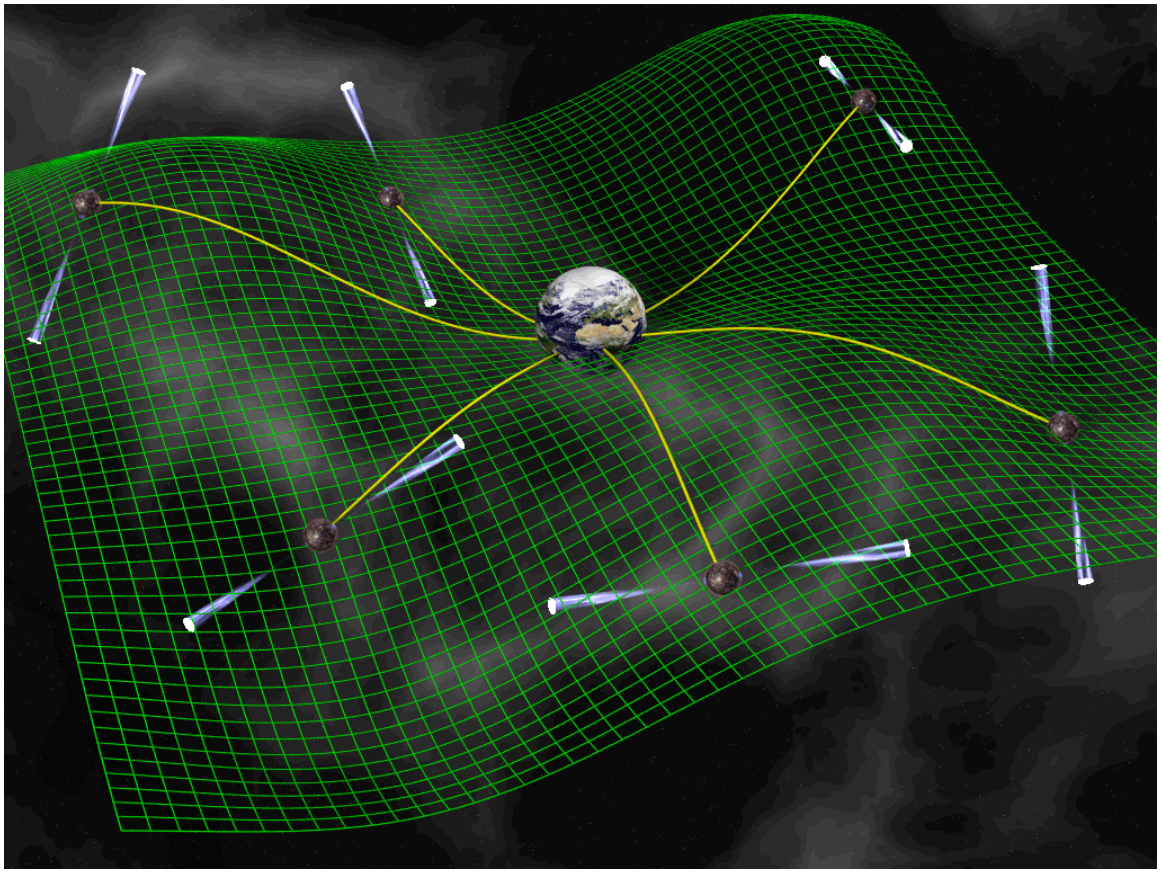

Distant pulsars send regular radio pulses – highly accurate clocks.
A passing gravitational wave would change the arrival time of the pulse.

Numerous collaborations around the world. Interesting upper limits and likely detections in the near future.

arXiv:1211.4590

Polarization Map of the Cosmic Microwave Background

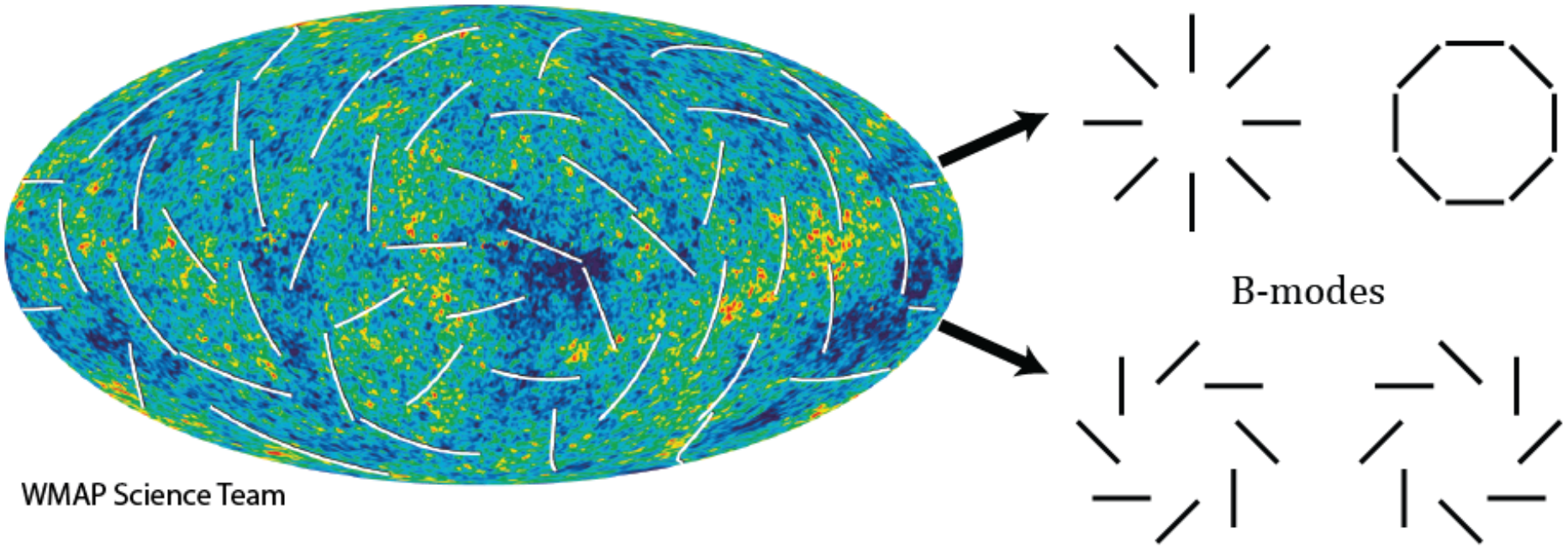

The CMB anisotropy polarization map may be decomposed into curl-free even-parity E-modes and divergence-free odd-parity B-modes.

Gravitational waves in the early universe imparts a “curl” on CMB polarization.
arXiv:1407.2584

Third Generation Gravitational Wave Detectors

Einstein Telescope

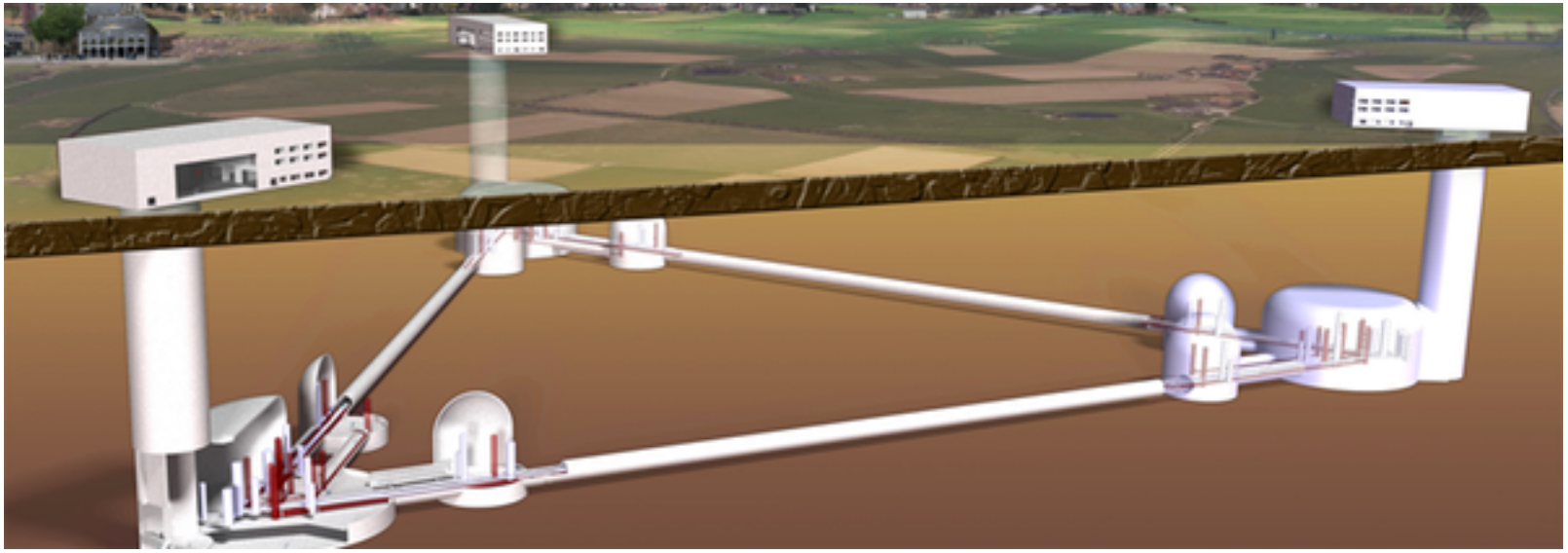

Underground to reduced seismic noise.
10 km arms
Cryogenic mirrors
Lower frequency limit – 1 Hz
10 x better sensitivity than 2nd generation detectors
Farther back in the universe

Third Generation Gravitational Wave Detectors

With Einstein Telescope (European) or Cosmic Explorer (US) almost every stellar mass binary black hole merger in the observable universe will be detectable.

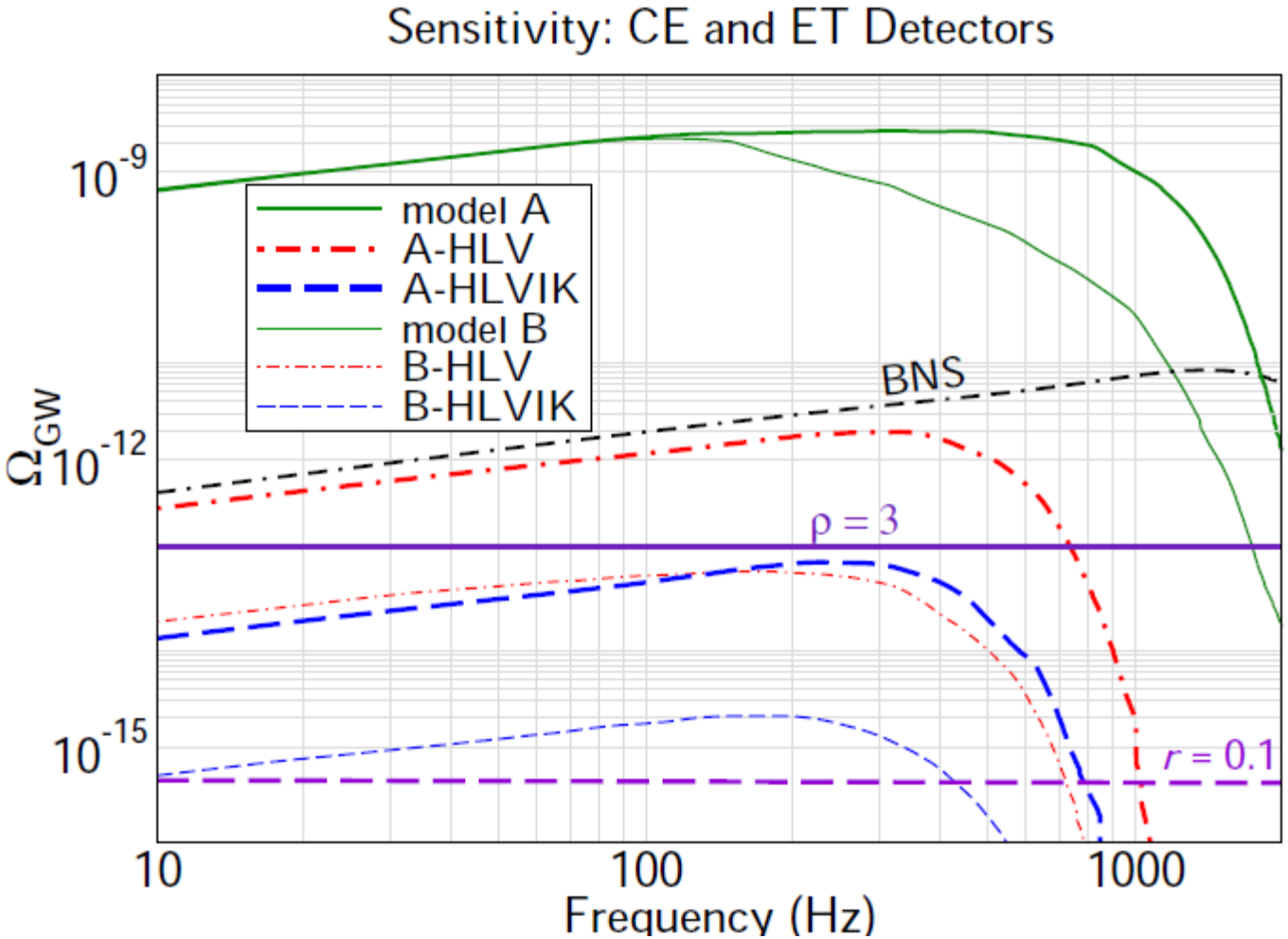

BBH confusion background can potentially be subtracted to observe the primordial background at the level of $\Omega_{GW} \sim 10^{-13}$ after five years of observation.

Arxiv:1611.08943

Atom Interferometers

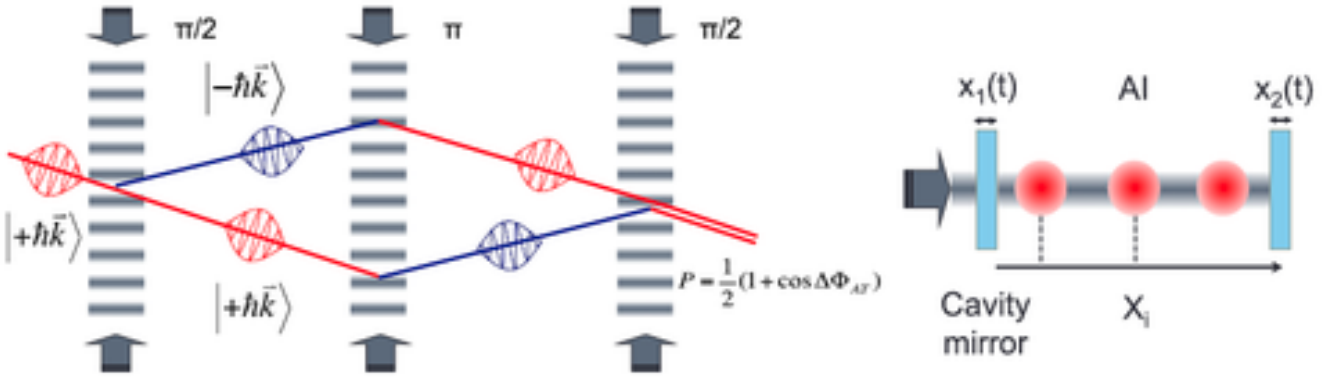

Use a long optical cavity to interrogate atom interferometers.

It may be possible to use this method to build a gravitational wave detector in the 0.1 Hz – 10 Hz band, between LISA and LIGO-Virgo.

Arxiv 1505:07137

Stochastic Gravitational Wave Background Sources

Typical Landscape

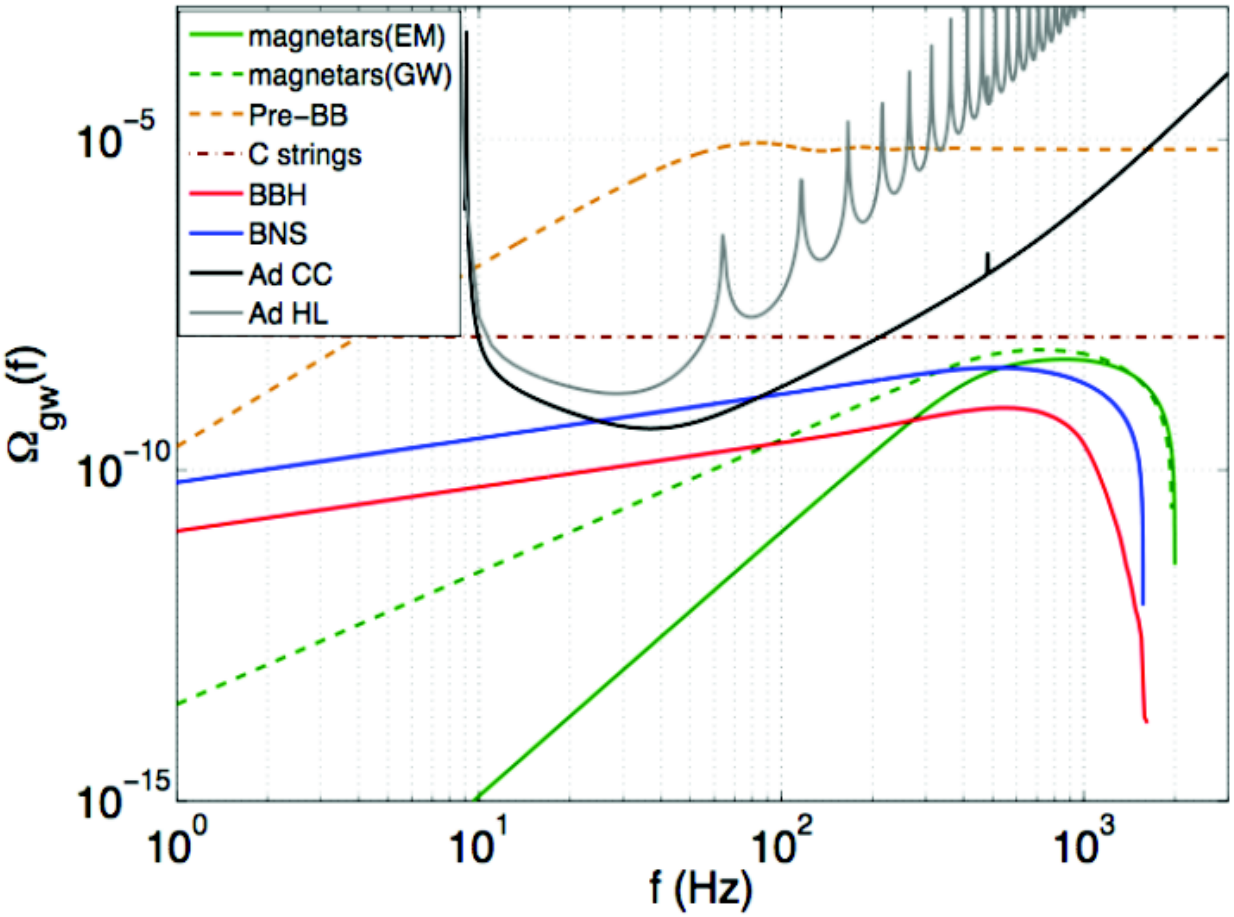

GW online plotter, Wu, Mandic, Regimbau, http://homepages.spa.umn.edu/~gwplotter/

Review of sources: T. Regimbau, arXiv 1101.2762

Cosmological Sources

- Standard inflation => stochastic background with small Ω_{GW}
- Other models readily accessible
- Cosmic strings
- Pre Big Bang models / String cosmology
- LIGO-Virgo will be probing energy scales of 10^9 – 10^{10} GeV in early universe
  - Well past limits of the standard model

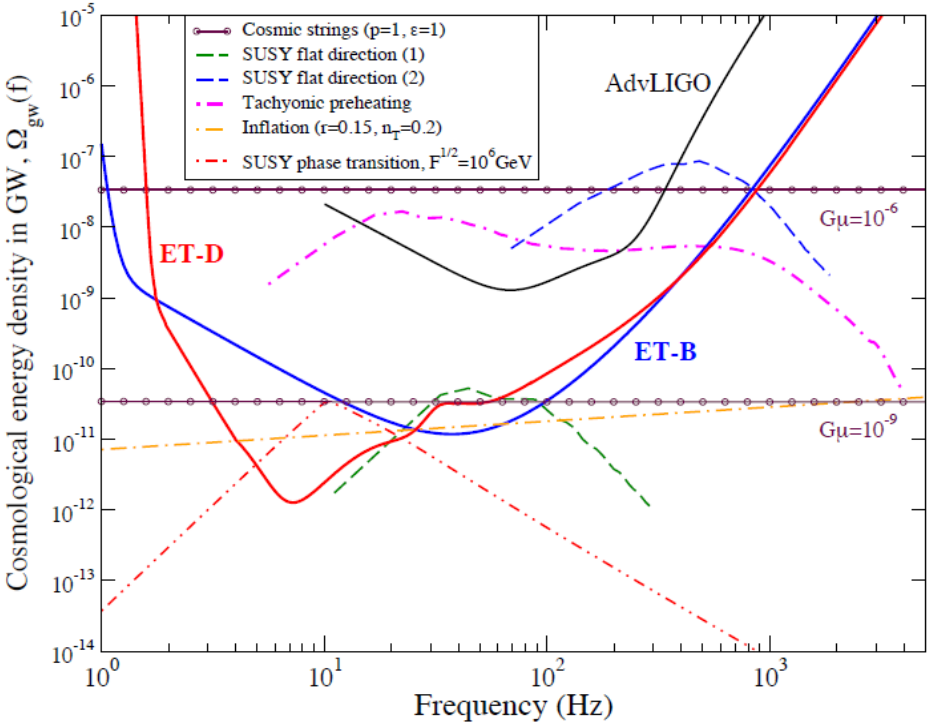

Plot from Einstein Gravitational Wave Telescope Instrument Design Study

Non-Standard Inflation

- Axion production => inflationary GW signals detectable by aLIGO

  (Ω_{GW} ~10^{-9} at 100 Hz) corresponding to energies of ~10^{17} GeV

  see N. Barnaby *et al.*, PRD **85**, 023525 (2012)

  J. Cook and L. Sorbo, PRD **85**, 023534 (2012)

- Inflation models ending in first order phase transitions => GWs from bubble collisions of the true vacuum phase. Could produce signals as large as

  Ω_{GW} ~10^{-8} at 100 Hz.

  See A. Lopez and K. Freese, arXiv:1305.5855

More Cosmological Sources for LIGO-Virgo

- Gravity Waves from Tachyonic Preheating after Hybrid Inflation; J-F Dufaux, GN. Felder, L Kofman, O Navros, arXiv:0812.2917
- Gravitational Waves from the Non-Perturbative Decay of Condensates along Supersymmetric Flat Directions; J-F Dufaux, arXiv:0902.2574
  - GWs from the decay of SUSY scalar fields
- Particle production during inflation and gravitational waves detectable by ground-based interferometers; JL Cook, L. Sorbo, arXiv:1109.0022
  - Particle production during inflation
- Relating gravitational wave constraints from primordial nucleosynthesis, pulsar timing, laser interferometers, and the CMB: implications for the early universe; LA Boyle, A Buonanno arXiv:0708.2279
  - Stiff equation of state after inflation
- Gravitational waves from self-ordering scalar fields; E Fenu, DG Figueroa, R Durrer, J Garcia-Bellido, arXiv:0908.0425
  - Scalar field relaxation

Astrophysical Sources

- Production of the SGWB from the start of stellar activity
- Background from inspiral of compact binary systems through the history of the universe
- Background from supernovae, neutron stars, magnetars.
- Astrophysical background falls nicely into observation band for advanced LIGO and advanced Virgo

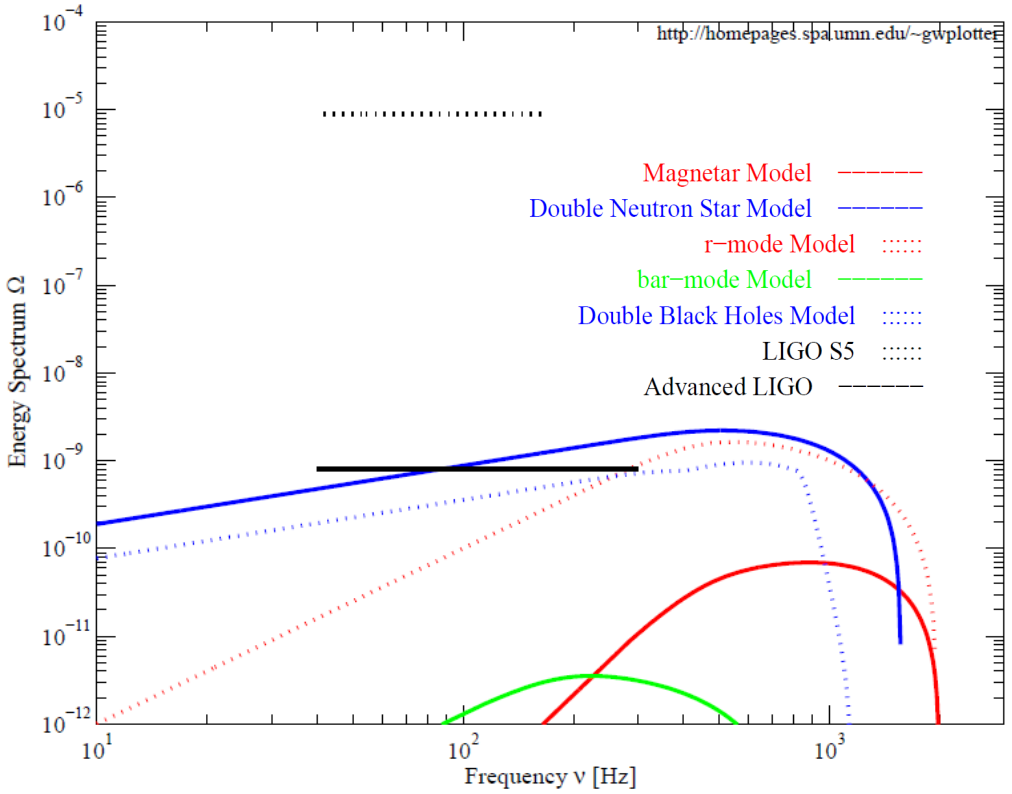

Astrophysical Sources

- Production of the SGWB from the start of stellar activity
- Background from inspiral of compact binary systems through the history of the universe
- Background from supernovae, neutron stars, magnetars.
- Astrophysical background falls nicely into observation band for advanced LIGO and advanced Virgo

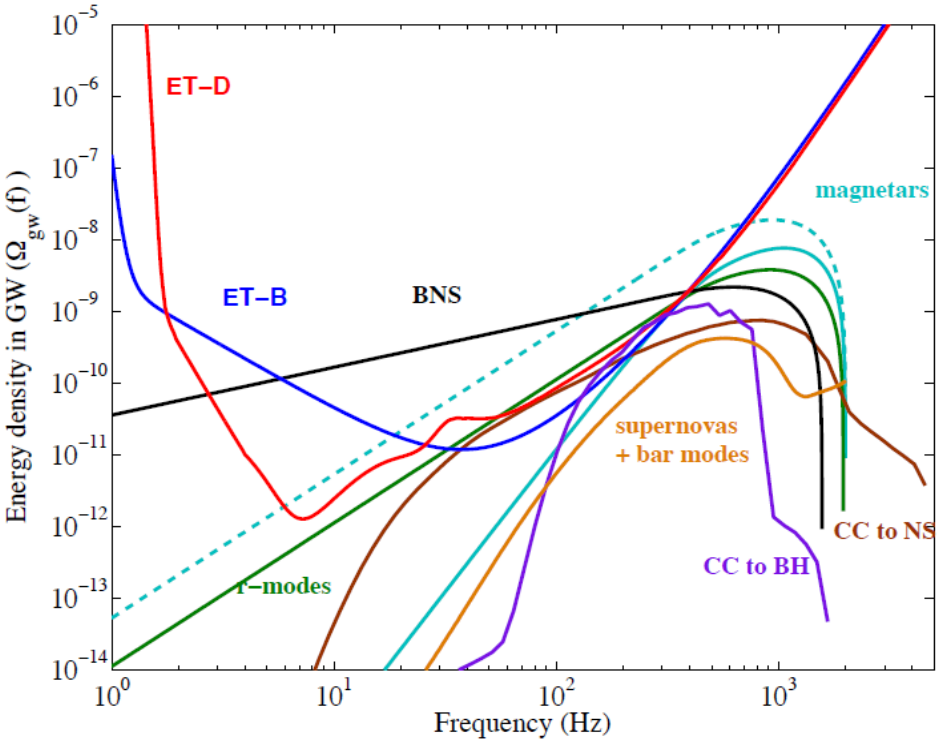

Plot from Einstein Gravitational Wave Telescope
Instrument Design Study

See C. Wu, V. Mandic, T. Regimbau, PRD **85** 104024 (2012), PRD **87** 042002 (2013)

Gravitational Wave Spectrum

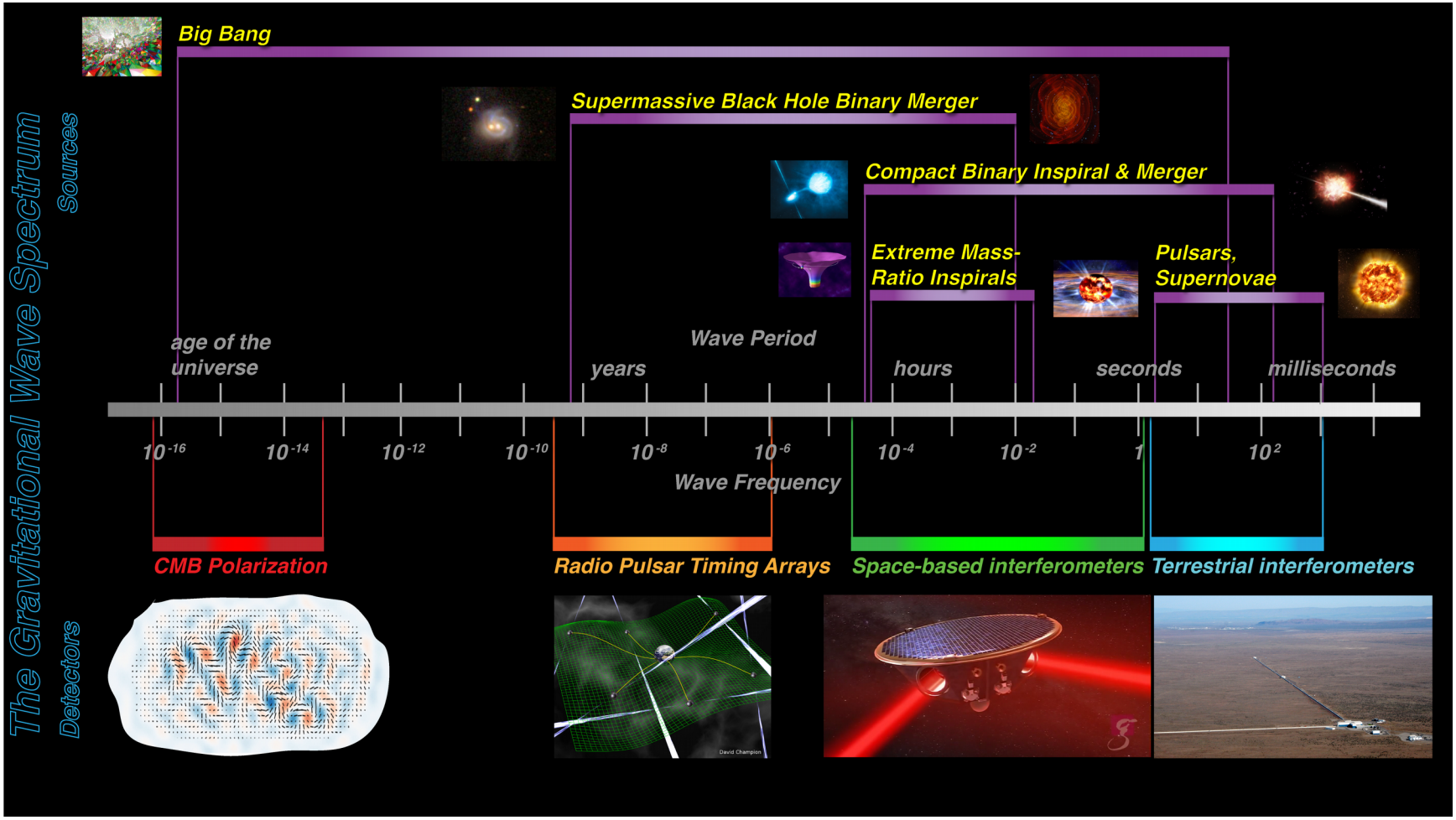

Laser Interferometer Space Antenna - LISA

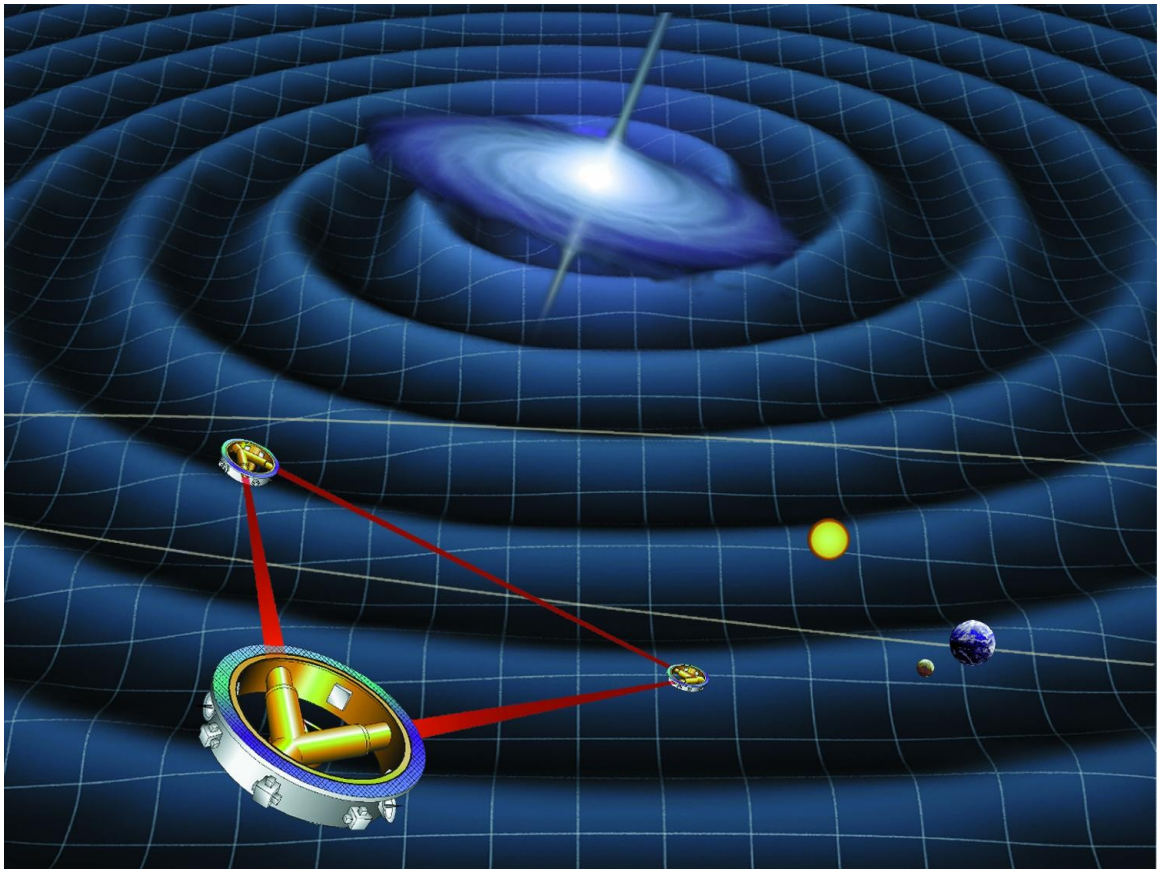

LISA physics

- the nature of gravity
- the fundamental nature of black holes
- black holes as sources of energy
- nonlinear structure formation
- dynamics of galactic nuclei
- formation and evolution of stellar binary systems
- the very early universe
- cosmography (specifically, the cosmic distance scale)

Gravitational Observatory Advisory Team – GOAT (ESA web site)

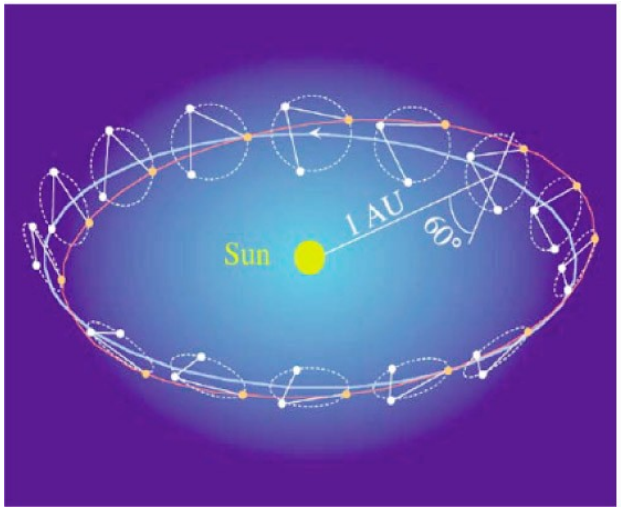

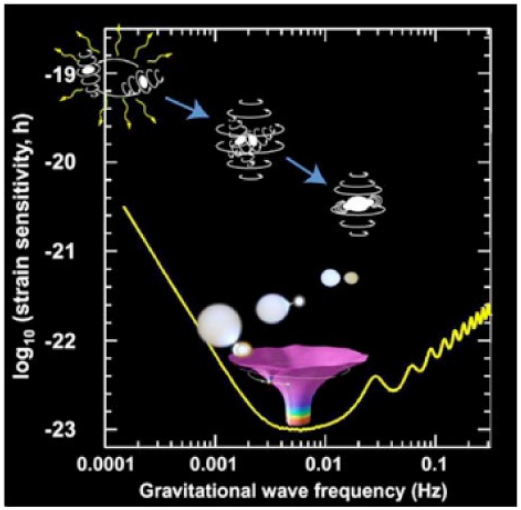

LISA Pathfinder – Demonstrating LISA Technology

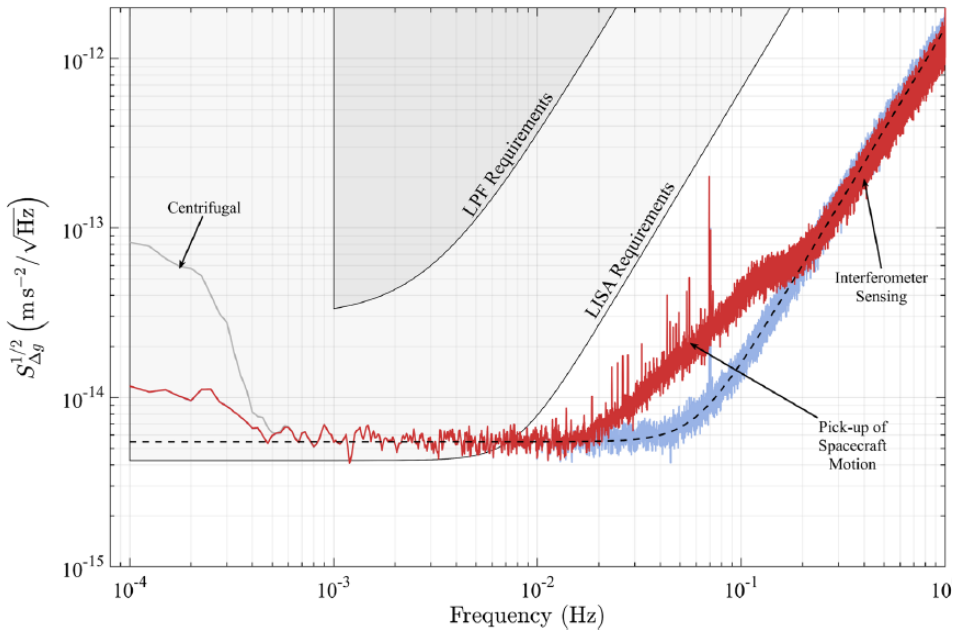

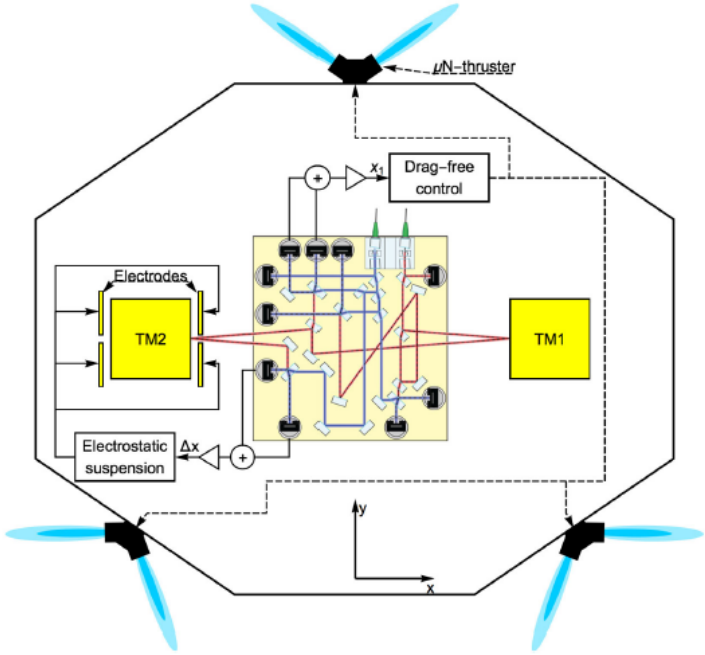

A set of cold gas micro-newton thrusters to ensure the spacecraft follows TM1. A second control loop forces TM2 to stay at a fixed distance from TM1 and thus centered in its own electrode housing.

LISA Proof Masses, Optical Bench, Interferometry and Telescopes

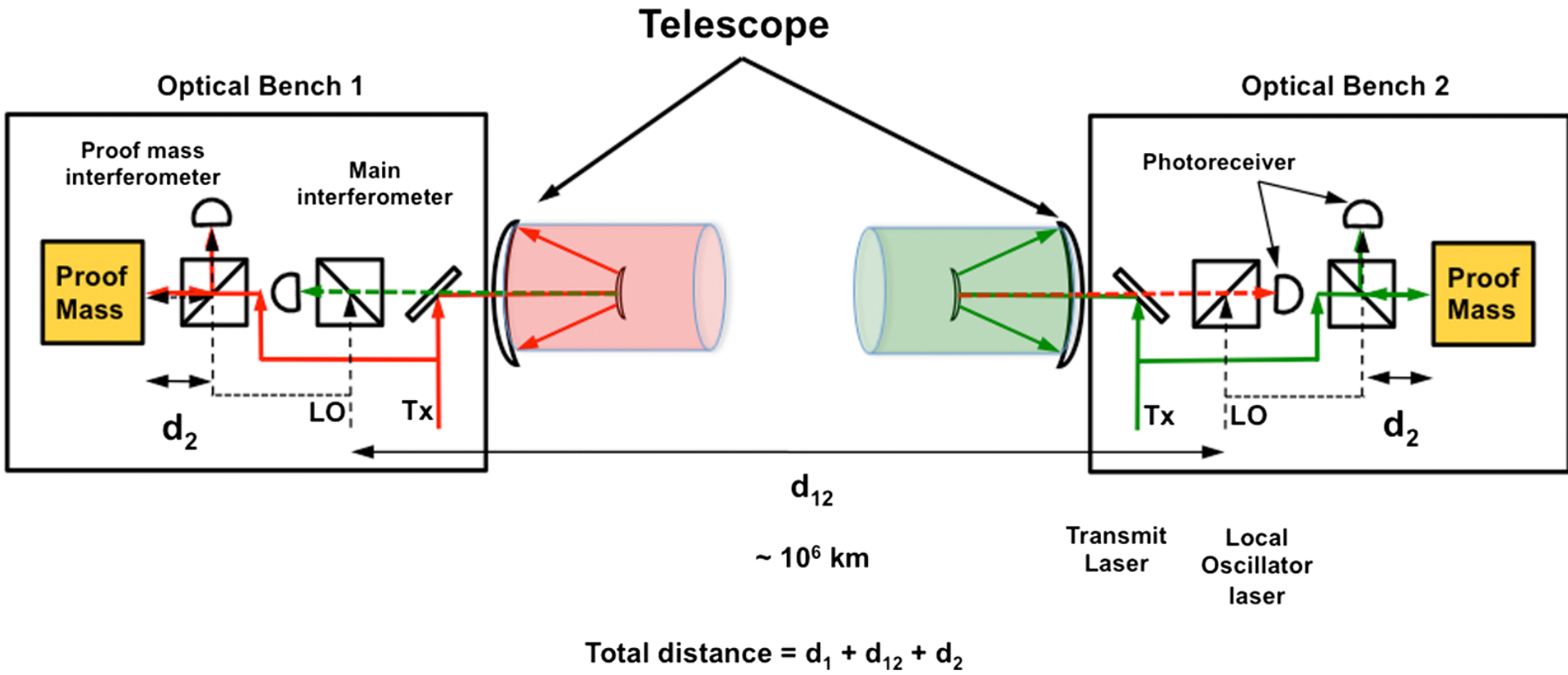

LISA Physics

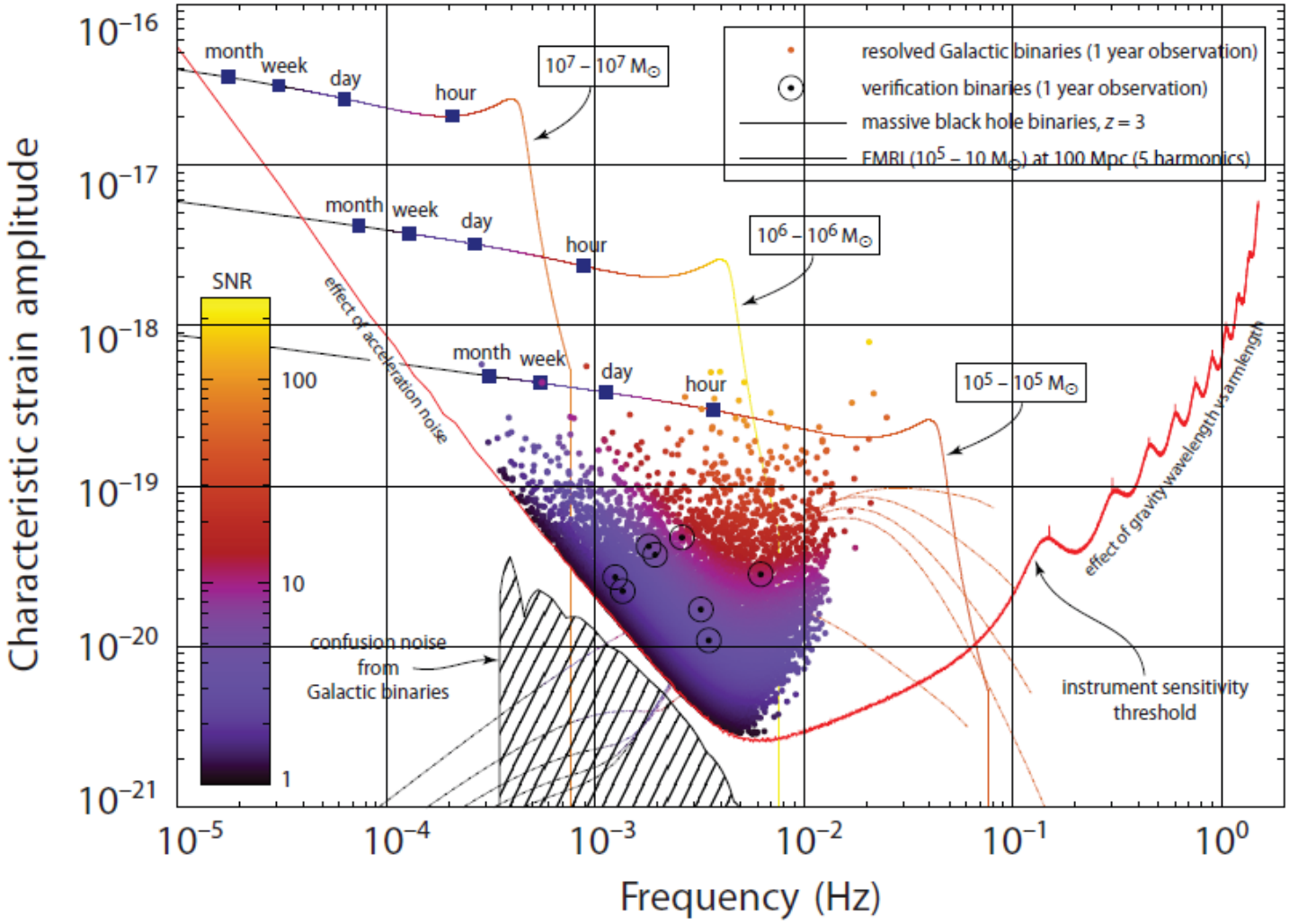

LISA Physics

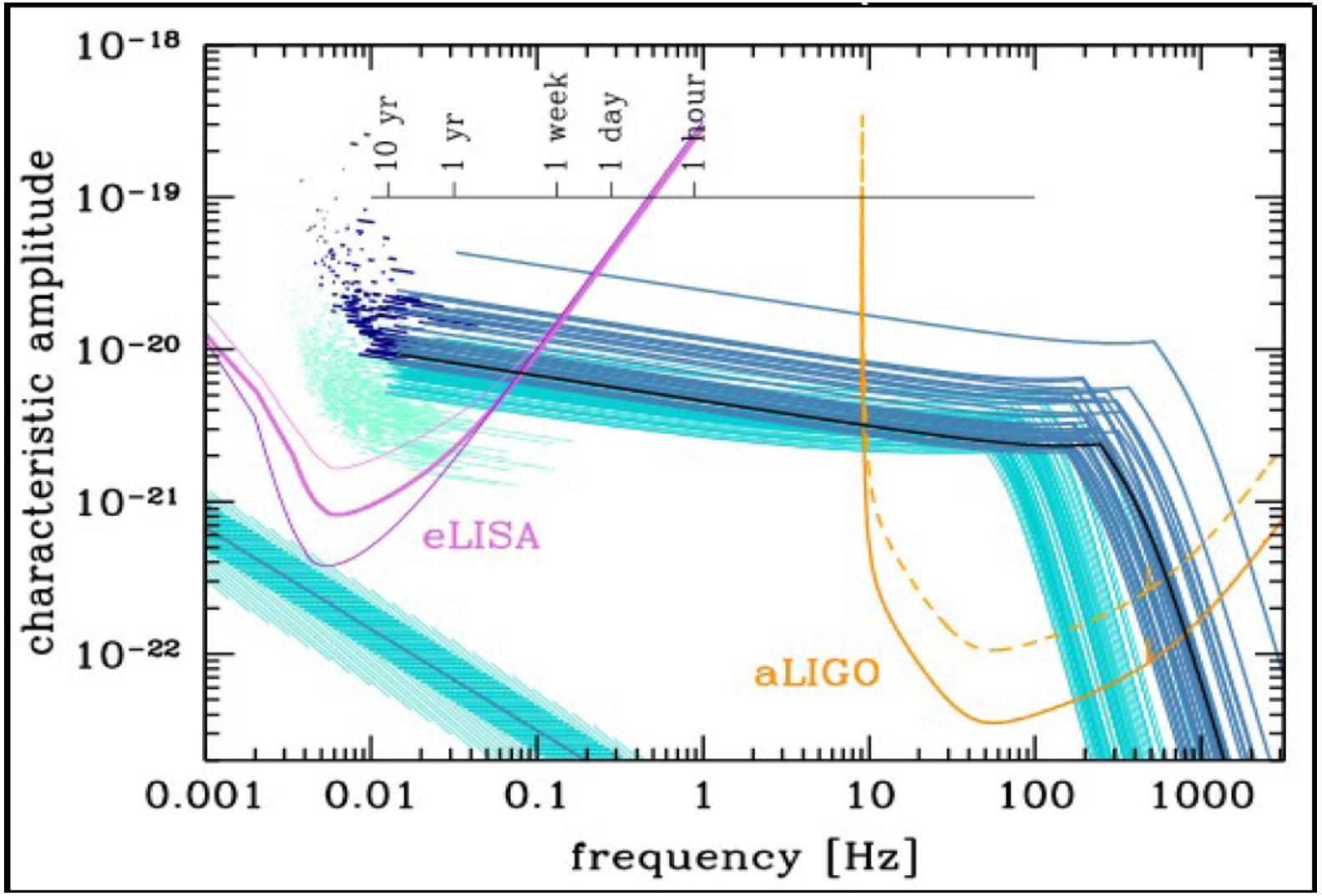

Gravitational wave signals from a heavy stellar black hole binaries. BBH systems can be observed by both LISA and Advanced LIGO – Advanced Virgo.

Testing the Early Universe

-
-
-

LISA Summary

The LISA project is presently moving forward rapidly.

ESA and NASA see this as a high priority.

A tremendous amount of R&D still needs to be done for LISA, and there is much experimental activity.

After the LHC, LISA may offer the best opportunity to observe the high energy physics that describes the universe.

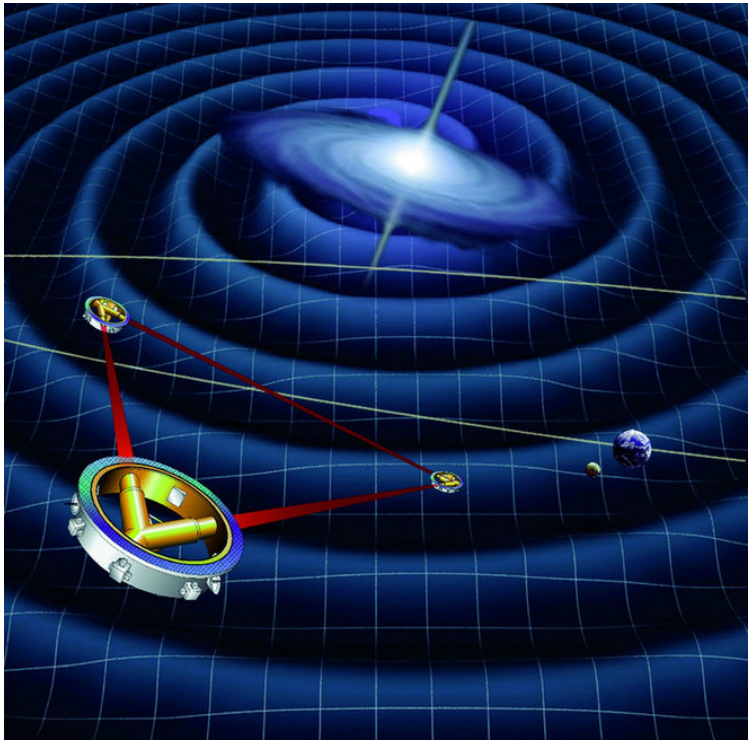

References and Further Reading

- "Measuring the Stochastic Gravitational Radiation Background with Laser Interferometric Antennas" N. Christensen, Physical Review D, Vol. 46, p. 5250 (1992).
- "Sensitivity of the Laser Interferometer Gravitational Wave Observatory to a stochastic background, and its dependence on the detector orientations", Eanna E. Flanagan, Phys. Rev. D Vol. 48, 2389 (1993).
- "Optimal detection strategies for measuring the stochastic gravitational radiation background with laser interferometric antennas" N.L. Christensen, Physical Review D, Vol. 55, p. 448-454 (1997).
- "Detecting a stochastic background of gravitational radiation: Signal processing strategies and sensitivities", B. Allen, J. Romano, Phys. Rev. D Vol. 59 102001 (1999).
- "Analysis of first LIGO science data for stochastic gravitational waves", B. Abbott et al., Phys. Rev. D Vol. 69 122004 (2004).
- "Gravitational waves. Vol 1, Theory and Experiments", M. Maggiore, Oxford, (2008).
- “GW150914: Implications for the Stochastic Gravitational-Wave Background from Binary Black Holes”, B. P. Abbott et al., Phys. Rev. Lett. Vol. 116 131102 (2016)
- "Detection methods for stochastic gravitational-wave backgrounds: a unified treatment", Joseph D. Romano, Neil. J. Cornish, Living Rev Relativ (2017) 20: 2.
- “Upper Limits on the Stochastic Gravitational-Wave Background from Advanced LIGO’s First Observing Run”, B. P. Abbott et al. Phys. Rev. Lett. Vol. 118 121101 (2017).
- Directional Limits on Persistent Gravitational Waves from Advanced LIGO’s First Observing Run, B. P. Abbott et al., Phys. Rev. Lett. Vol. 118 121102 (2017)

Extra Slides

Noise Lines In LIGO O1 Data

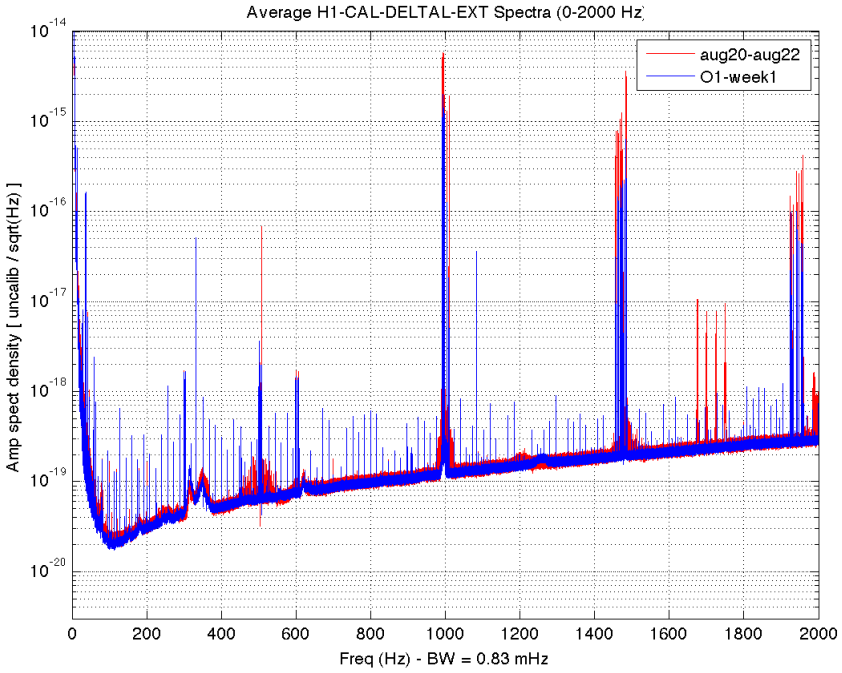

Noise Power Spectral Density H1 in O1

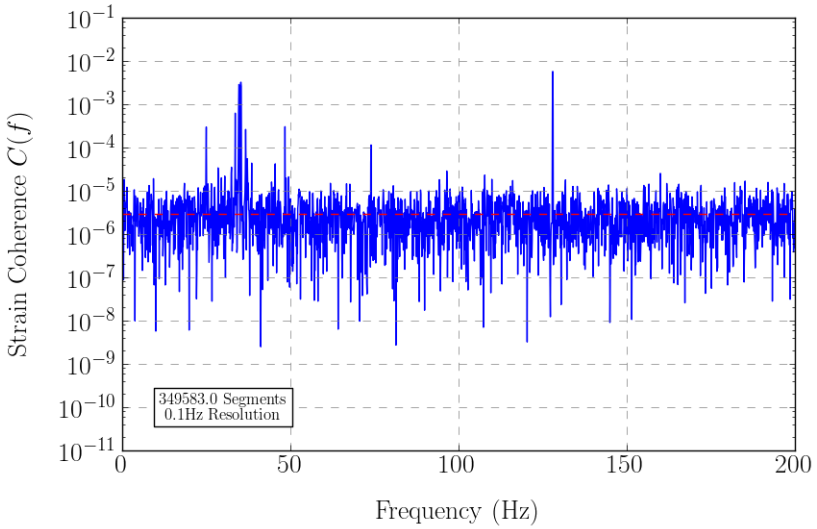

H1-L1 O1 Coherence

Common noise – similar equipment.
Bin size switched to 1/32 Hz for notching; nominally 0.25 Hz.

O1 Sensitivity to $\Omega_{gw}(f)$ Through the Observing Run

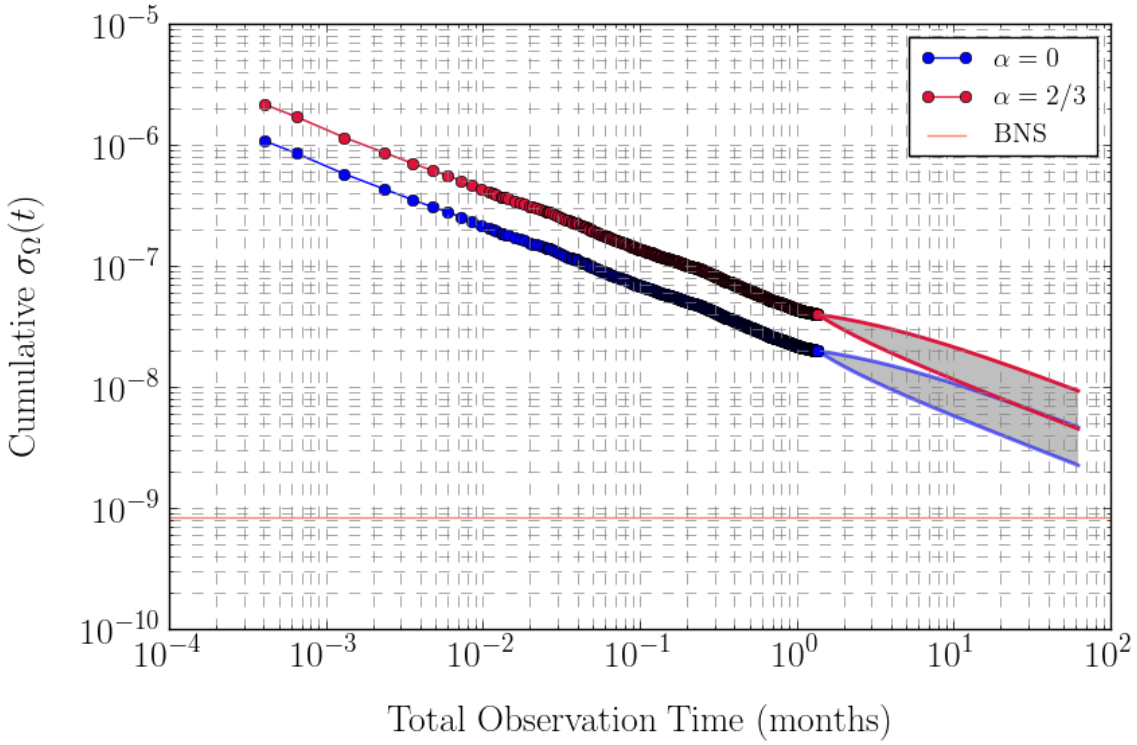

Integrated broadband search sensitivity σ(t) and 5 year predicted sensitivity vs cumulative observation time for a flat spectrum (α=0, blue) and for an astrophysical spectrum (α=2/3, red). The solid lines show the predicted future evolution of σ, achieved by extrapolating using the mean hourly sensitivity (upper bounds) and the best hourly sensitivity (lower bounds). The orange line represents the astrophysical prediction for the BBH/BNS background at 100Hz.

Advanced LIGO – Advanced Virgo

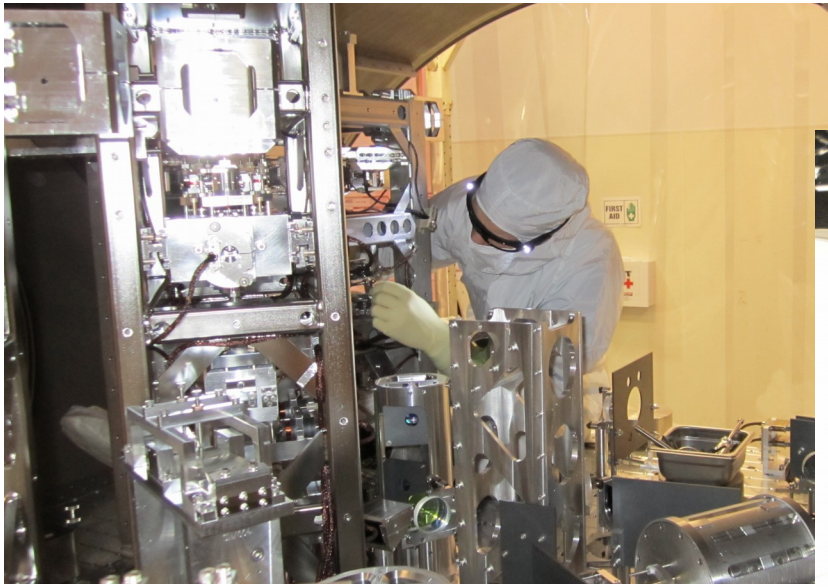

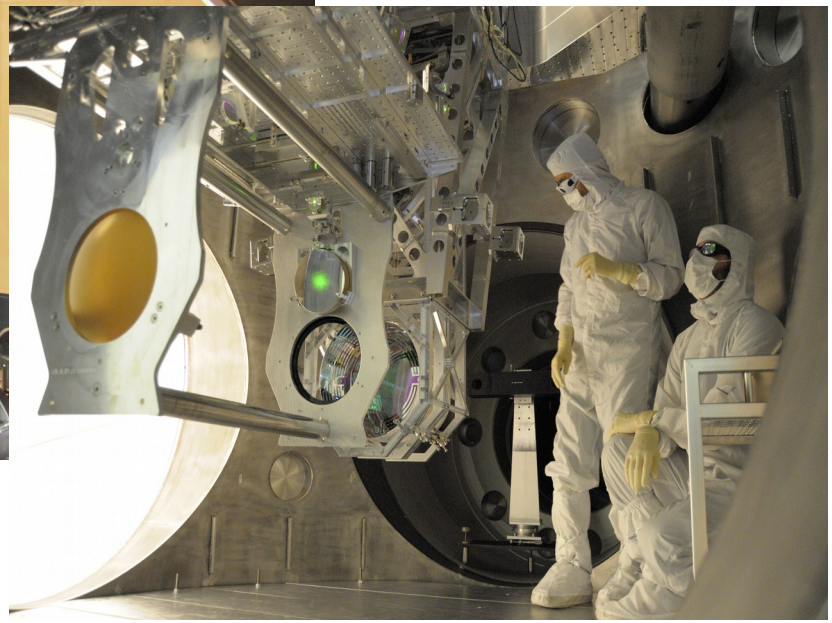

Built on the experience gained from the first generation (2004 - 2010) detectors

Advanced LIGO

- Initial LIGO: 2005-2010.
- Advanced LIGO commissioned 2010-2015.
  - » Increased laser power
  - » Sophisticated seismic/vibration suppression
  - » Quadruple pendula suspensions
  - » Larger mirrors, better suspension material
  - » More complex and versatile interferometer configuration.

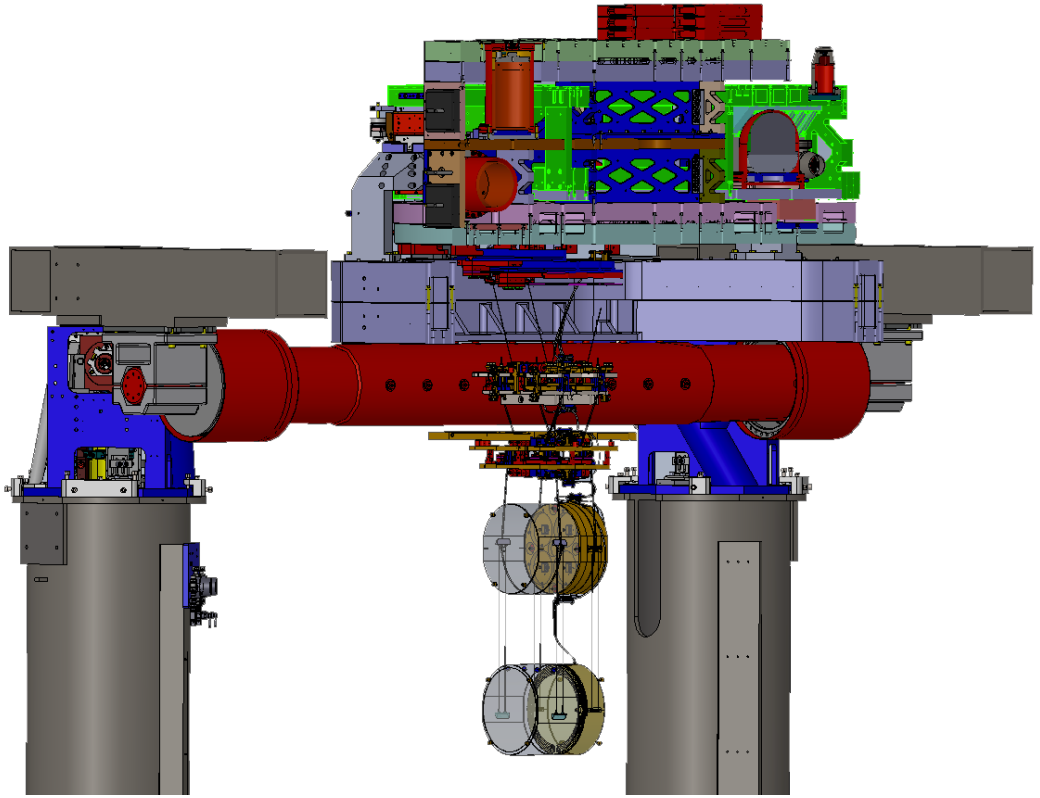

O2, second observing run, started last fall, goes to August.

Advanced Virgo

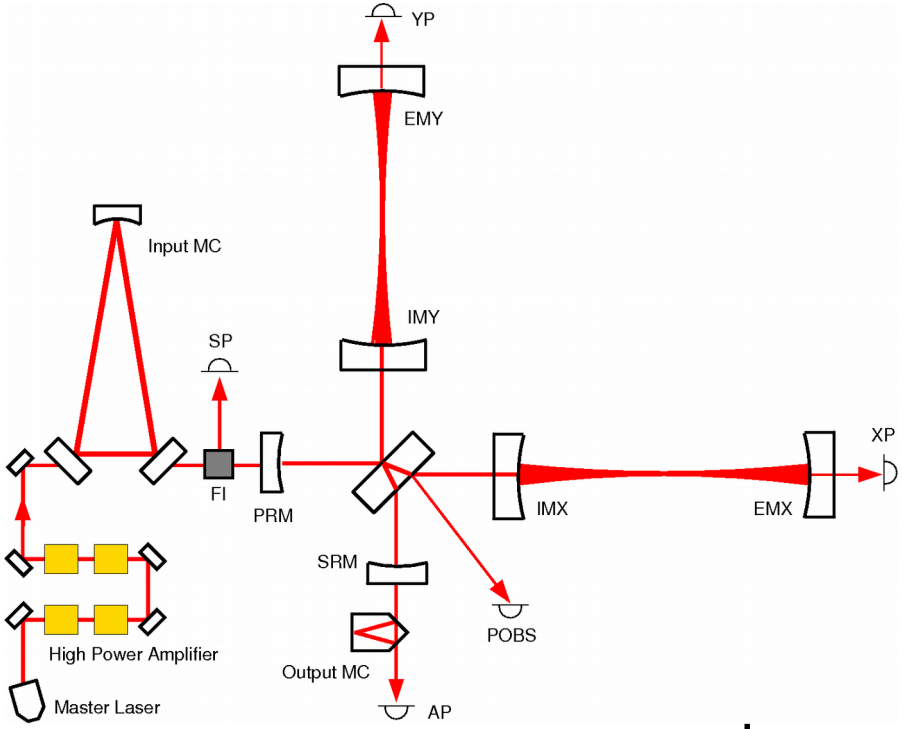

- Larger mirrors; better optical quality.
- Higher finesse of the arm cavities
- Increased laser power.
- Coming on-line in Spring 2017 to join O2.

Black Hole Population

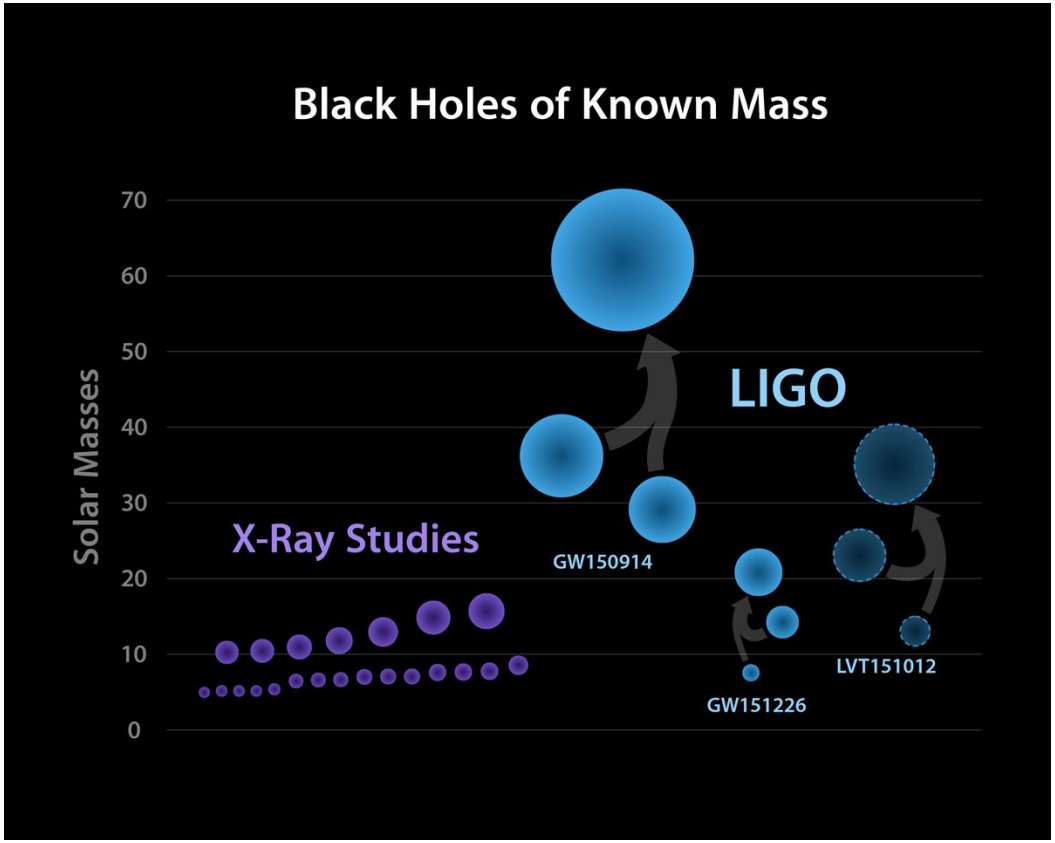

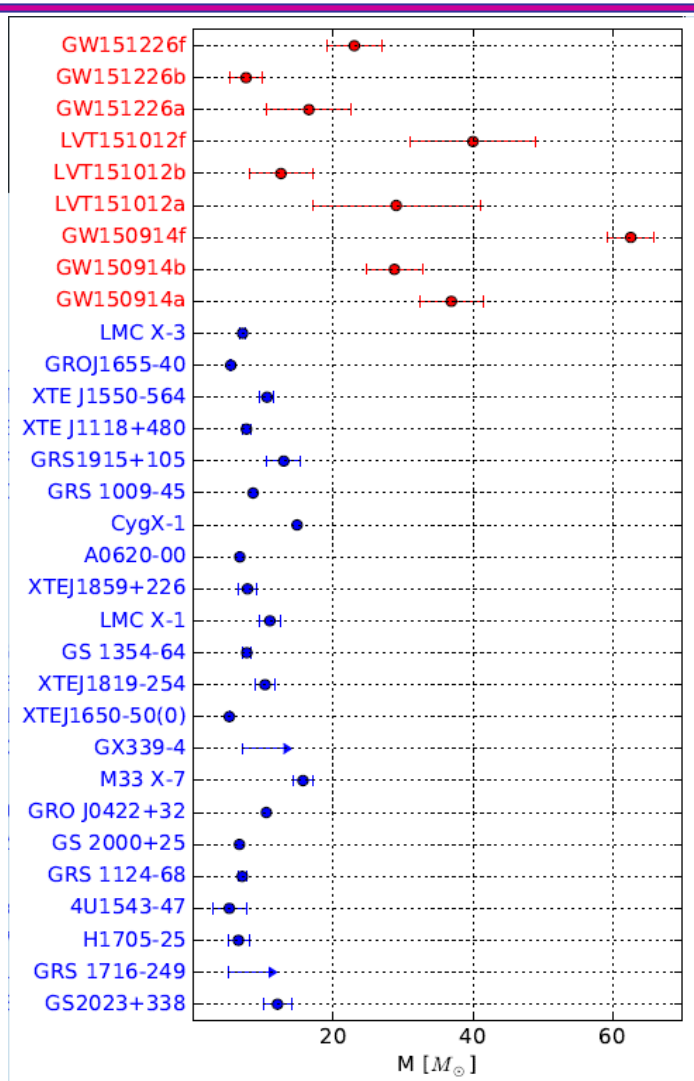

Image Credit LIGO

Binary Black Hole Merger Rate

•Assuming that all binaries are like these 3 events is not realistic.

•Try two alternative models:

Flat distribution in log m1 – log m2

- (m1) $\propto m_1^{-2.35}$ with a uniform distribution for the second mass.

• Significantly different rate estimates.

• Altogether: 9 – 240 Gpc^{-3} yr^{-1}.

• Lower limit comes from the flat in log mass population and the upper limit from the power law population distribution.

• Rules out <9 Gpc^{-3} yr^{-1}, which were previously allowed.

Stochastic Gravitational-wave Background

A stochastic background of gravitational waves results from the superposition of a large number of independent unresolved sources at different stages in the evolution of the Universe.

- **Cosmological:** signature of the early Universe near the Big Bang *inflation, cosmic strings, phase transitions…*
- **Astrophysical:** since the beginning of stellar activity : *compact binary coalescences, core-collapse supernovas, rotating neutron stars, capture by SMBHs…*
- **What do we try to measure?**

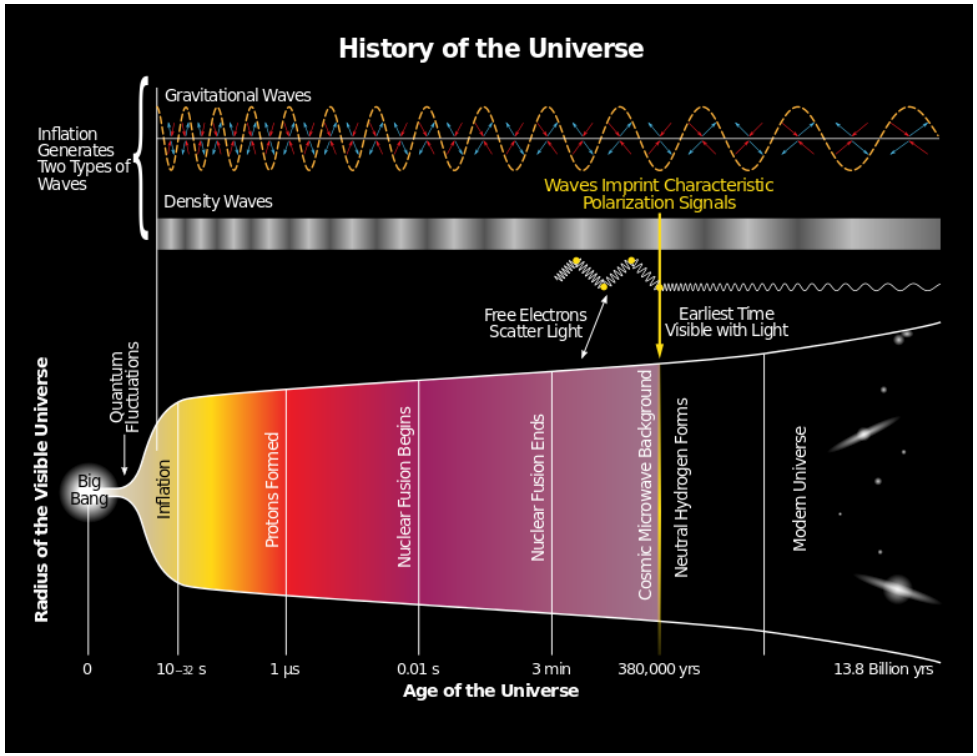

$$\Omega_{GW}(f) = \frac{f}{\rho_c}\frac{d\rho_{GW}}{df} \qquad \Omega_{GW}(f) = A(f/f_{ref})^{\alpha}$$

Gravitational Wave Spectrum